From Blue Azulenes to Blue Heptalenes – New Strongly Polarized π-Convertible Heptalenes

by **Thomas Landmesser**[1]), **Anthony Linden**, and **Hans-Jürgen Hansen***

Organisch-chemisches Institut der Universität Zürich, Winterthurerstrasse 190, CH-8057 Zürich (phone: +41-44-6354231; fax: +41-44-6356833; e-mail: hjhansen@oci.uzh.ch)

The 1,5,6,8,10-pentamethylheptalene-4-carboxaldehyde (**4b**) (together with its double-bond-shifted (DBS) isomer **4a**) and methyl 4-formyl-1,6,8,10-tetramethylheptalene-5-carboxylate (**15b**) were synthesized (*Schemes 3* and *7*, resp.). Aminoethenylation of **4a**/**4b** with *N*,*N*-dimethylformamide dimethyl acetal (=1,1-dimethoxy-*N*,*N*-dimethylmethanamine = DMFDMA) led in DMF to 1-[(1*E*)-2-(dimethylamino)ethenyl]-5,6,8,10-tetramethylheptalene-2-carboxaldehyde (**18a**; *Scheme 9*), whereas the stronger aminoethenylation agent *N*,*N*,*N*′,*N*′,*N*″,*N*″-hexamethylmethanetriamine (=tris(dimethylamino)methane = TDMAM) gave an almost 1:1 mixture of **18a** and 1-[(1*E*)-2-(dimethylamino)ethenyl]-5,6,8,10-tetramethylheptalene-4-carboxaldehyde (**20b**; *Scheme 11*). Carboxylate **15b** delivered with DMFDMA on heating in DMF the expected aminoethenylation product **19b** (*Scheme 10*). The aminoethenylated heptalenecarboxaldehydes were treated with malononitrile in CH_2Cl_2 in the presence of $TiCl_4$/pyridine to yield the corresponding malononitrile derivatives **23b**, **24b**, and **26a** (*Schemes 13* and *14*). The photochemically induced DBS process of the heptalenecarboxaldehydes as 'soft' merocyanines and their malononitrile derivatives as 'strong' merocyanines of almost zwitterionic nature were studied in detail (*Figs. 10–29*) with the result that 1,4-donor/acceptor substituted heptalenes are cleaner switchable than 1,2-donor/acceptor-substituted heptalenes.

1. Introduction. – In the foregoing publication, we reported in detail on the synthesis as well as on the UV/VIS behavior of π-convertible methyl heptalenecarboxylates of type **A** and **B** with phenyl capped (*E*)-ethenyl and (1*E*,3*E*)-buta-1,3-dien-1-yl residues in 2,5- and 1,4-position, respectively (*Scheme 1*; see [1] and our former publications cit. therein). The introduction of MeO (or Me_2N) and NO_2 substituents in 4-position of the phenyl groups led in the **B** forms to through-conjugated merocyanine systems with strong absorption enhancement of the longest-wavelength heptalene band I with λ_{max} values in the range of the corresponding linear (all-*E*)-polyenes (*cf.* Fig. 23 in [1]). In the present work, we tried to shift the absorption maximum of the heptalene band I of the through-conjugated **B** forms to longer wavelengths with concomitant enhancement of their absorption intensity. To do so, we decided to take 6,8,10-trimethylheptalenes as basic part for our investigations in view of their higher thermal stability with respect to the cyclic double-bond shifts (DBS), which establish the equilibrium **A** $\rightleftharpoons$ **B**. Moreover, we chose the (1*E*)-2-(dimethylamino)ethenyl group as $\pi(1)$ substituent, since this group can easily be introduced in dimethyl 1-

[1]) Part of the Ph.D. thesis of *T. L.*, University of Zurich, 2001; current address: *Siegfried AG*, Untere Brühlstrasse 4, CH-4800 Zofingen.

Scheme 1

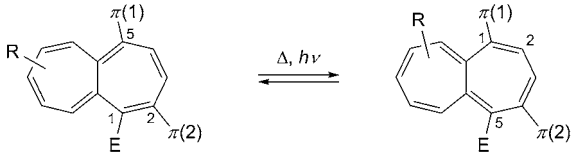

A **B**

$\pi(1)$ = 4-$XC_6H_4[CH{=}CH]_m$; X = MeO, Me_2N, NO_2
$\pi(2)$ = 4-$YC_6H_4[CH{=}CH]_n$; Y = NO_2, MeO
m, *n* = 1, 2
E = COOMe; R = alkyl

methylheptalene-4,5-dicarboxylates (*i.e.*, $\pi(2) = \text{COOMe}$) or methyl 1-methylheptalene-5-carboxylates with other electron-acceptor groups (CHO, CN, CH=CHCOOMe) at C(4) [2]. On the other hand, aldehydes can easily undergo reaction with the CH-acidic methylene group of malononitrile (**1**) or those of **2** and **3** derived from 1*H*-indene-1,3(2*H*)-dione with malononitrile (*Fig. 1*) to yield the corresponding ethene structures of merocyanines (see, *e.g.*, [3][4]) or methine dyes (see, *e.g.*, [5][6]). In some preliminary experiments, we tried to condense 1,5,6,8,10-pentamethylheptalene-2-carboxaldehyde (**4a**) in a mixture with its DBS isomer **4b** and **2** under typical *Knoevenagel* conditions (EtOH, piperidine, reflux) and found that the catalyst piperidine entered actively the reaction sequence, in a way that finally 2,9-dihydro-9-oxo-1-(1,5,6,8,10-pentamethylheptalen-2-yl)-3-(piperidin-1-yl)-1*H*-indeno[2,1-*c*]pyridine-4-carbonitrile (**5a**) was isolated as dark violet crystals, which in solution in the presence of air were slowly dehydrogenated to **6a** (*Scheme 2*), a process, which also could be realized easier with $KMnO_4$ in acetone[2]). We reported already about these transformations [7], which work quite generally with **2**, aromatic aldehydes, and secondary amines.

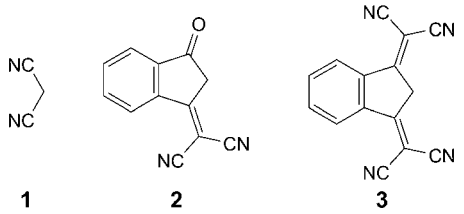

1 **2** **3**

Fig. 1. *Cyano-activated methylene compounds*

We restricted therefore our present investigations on heptalenecarboxaldehydes with the 2-(1*E*)-(dimethylamino)ethenyl group as $\pi(1)$ substituent and the transformation of their aldehyde group with **1** to a 2,2-dicyanoethenyl moiety as $\pi(2)$ substituent, which led in some cases to unexpected results.

---

[2]) We assumed that **3** would react with the aldehyde mixture **4a**/**4b** in a similar manner as **2**, whereby one of dicyanomethylidene groups of **3** would take the place of the oxo group at C(9) of **5a**. We did not check experimentally this possibility.

Scheme 2

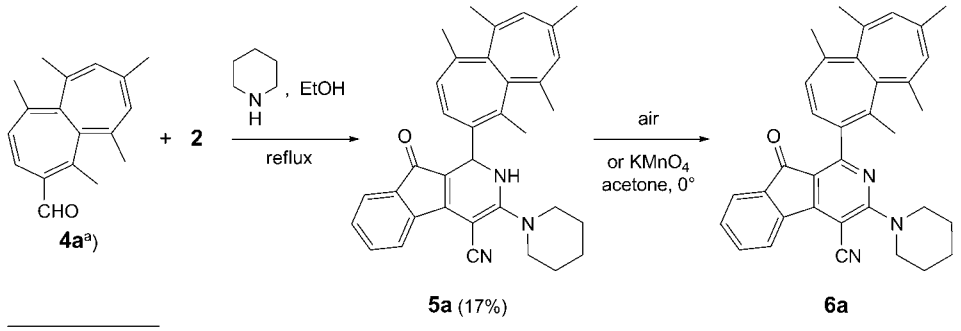

[a]) Mixture of **4a** (43%) and **4b** (57%).

2. Results and Discussion. – 2.1. *Synthesis of 6,8,10-Trimethylheptalenecarboxaldehydes. Knaup* and *Hafner* and co-workers [8] described an interesting acid-catalyzed, formally intramolecular disproportionation reaction of 1,6,8,10-tetramethylheptalene-4,5-dimethanol (**7b**), which was easily available by reduction of the corresponding dimethyl heptalenedicarboxylate with $LiAlH_4$ (see, *e.g.*, [9]). It yielded, by heating in boiling benzene in the presence of catalytic amounts of TsOH, 1,5,6,8,10-pentamethylheptalene-2-carboxaldehyde (**4b**) and its DBS isomer **4a** as well as small amounts of 2,5,6,8,10-pentamethylheptalene-1-carboxaldehyde (**8**) (*Scheme 3*). We could not realize the yields reported in [8][3]) but found that reliable high yields of the DBS mixture **4a**/**4b** could be obtained by heating **7b** in boiling 1,4-dioxane in the presence of 10 mol-% TsOH. Unfortunately, we found no conditions for the separation of practicable amounts of the DBS mixture by column chromatography. Nevertheless, the by-product **8**, formed in amounts $< 6\%$, could be separated from **4a**/**4b** by column chromatography (CC; silica gel). This procedure gave the pure DBS mixture with 57% of **4b** and 43% of **4a**. All further experiments were performed with this mixture.

Scheme 3

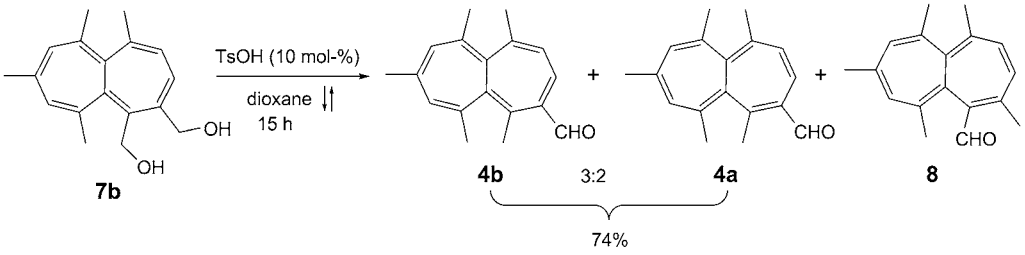

[3]) In boiling benzene, we got only 21% of the DBS mixture **4a**/**4b**, accompanied by 5% of **8**.

To get a bit more insight in the mechanism of the acid-catalyzed disproportionation reaction of **7b**, we synthesized 6,8,10-trimethylheptalene-1,4,5-trimethanol (**11b**) according to *Scheme 4*. The reaction of 1-(chloromethyl)-6,8,10-trimethylheptalene-4,5-dicarboxylate **9b** [1] with AcOK in DMSO at room temperature gave the corresponding 1-[(acetyloxy)methyl]heptalenedicarboxylate **10b** in an acceptable yield (*cf.* [10]). The latter was then reduced with diisobutylaluminium hydride (DIBAH) in THF at 0° under concomitant cleavage of the acetyloxy function.

Scheme 4

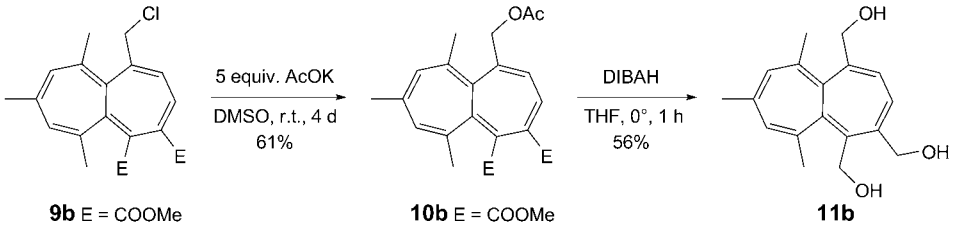

9b E = COOMe **10b** E = COOMe **11b**

In the case that vicinal hydroxymethyl groups as in **7b** are necessary for the observed intramolecular redox process leading to **4a**/**4b**, we expected the formation of 1-(hydroxymethyl)-5,6,8,10-tetramethylheptalene-4-carboxaldehyde (**12b**) and its DBS isomer (*Scheme 5*). Indeed, when we submitted **11b** to the optimized conditions for the disproportionation of **7b** (*Scheme 3*), we found in up to 20% yield a hydroxycarbonyl compound as stabile orange solid, which crystallized excellently, especially when recrystallized from Et_2O. Since **11b** is generally not very stable, we searched for better reaction conditions for **11b**. Finally, we found that short heating of **11b** in boiling diethylene glycol dimethyl ether (diglyme; 1,1′-oxybis[2-methoxyethane]) in the presence of catalytic amounts of TsOH gave **13b**, with difficulties to control yields of up to 39% (*Scheme 5*).

Scheme 5

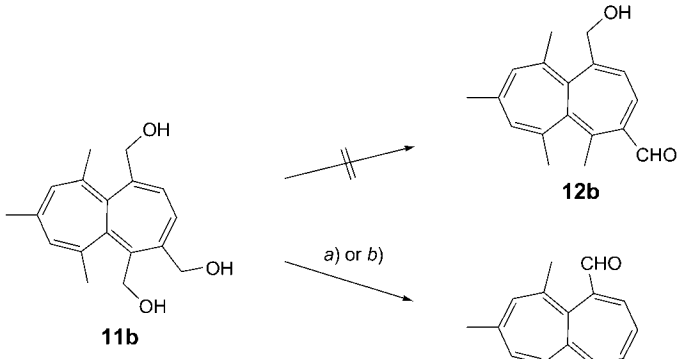

We solved the final structure of **13b** by an X-ray crystal-diffraction analysis, which showed no specific structural features in comparison with other highly substituted heptalene derivatives (*cf.* [11][12]). However, the monoclinic crystals of **13b** revealed an interesting packing pattern. The OH group of the molecule acts as a donor for intermolecular H-bonds. The corresponding acceptor is the aldehyde O-atom of a neighboring molecule (d(OH···O=C) = 189 pm). The molecules are linked thus in y-direction as infinite one-dimensional chains running along a 2_1 screw axis (*Fig. 2*). This intermolecular H-bonding may also explain the high tendency of **13b** for crystallization.

The structure of **13b** also points to the mechanistic nature of the acid catalyzed disproportionation reaction of **11b** as well as of **7b** (*Scheme 6*). Protonation of $HOCH_2$–C(5) followed by loss of H_2O generates tropylium ion **X1**, which isomerizes by a prototopic shift to **X2**. Deprotonation of **X2** leads to **13b**[4]).

Scheme 6

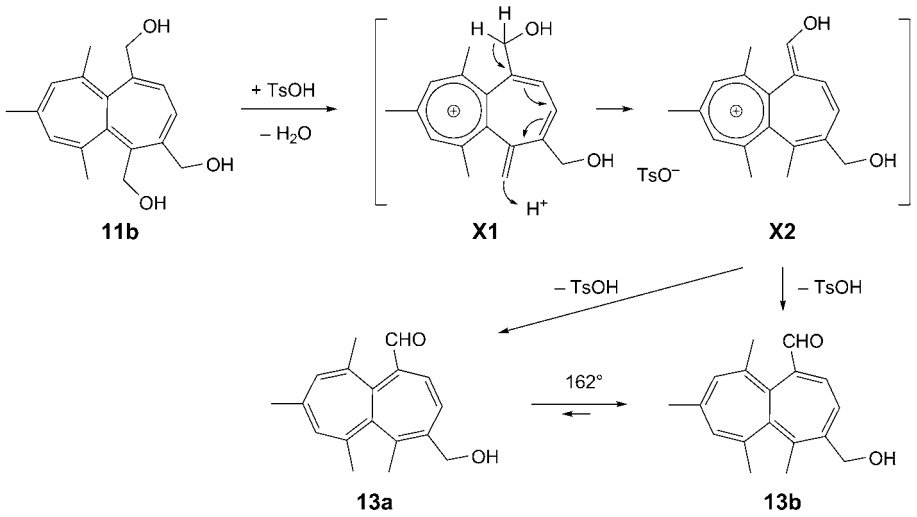

By reduction of 1,1-dimethoxy-6,7,9,11-tetramethylheptaleno[4,5-*c*]furan-3(1*H*)-one (**14b**) [13] with DIBAH in toluene (*cf.* [1]), we obtained methyl 4-formylheptalene-5-carboxylate **15b** as carboxylic ester analog of **4b** in good yield (*Scheme 7*).

2.2. *Formation of New Heptalene Based Merocyanines.* In our former work on donor–acceptor-substituted heptalenes [2], we treated 1-methylheptalene-4,5-dicarboxylates **16b** with *N*,*N*-dimethylformamide dimethyl acetal (=1,1-dimethoxy-*N*,*N*-dimethylmethanamine = DMFDMA) in hot DMF to get the corresponding 1-[(1*E*)-

---

[4]) The isomer **13a** was not found in isolable amounts. The temperature of boiling diglyme would be sufficient for a rapid DBS process. Indeed, AM1 calculations show that **13b** is by 3.8 kcal mol^{-1} more stable than **13a**. This means, taking $\Delta\Delta S_{435} \approx 0$, K_{435}(**13b**/**13a**) ≈ 99:1, in agreement with our finding.

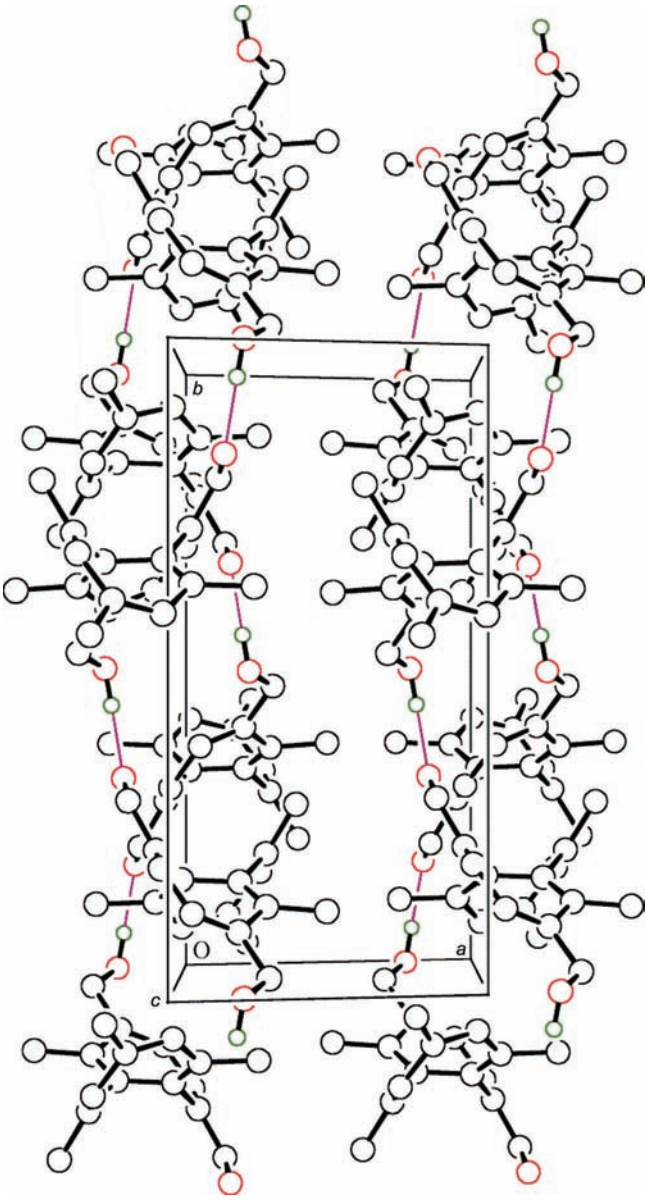

Fig. 2. *View of the crystal packing of 4-(hydroxymethyl)-5,6,8,10-tetramethylheptalene-1-carboxaldehyde* (**13b**). Sight on the screw axis formed by intermolecular H-bonding in the *y*-direction.

2-(dimethylamino)ethenyl]heptalene-4,5-dibarboxylates **17b** (*Scheme 8*), following thereby a procedure originally developed by *Batcho* and *Leimgruber* for functionalizing 2-nitrotoluenes in view of a new synthesis of indoles [14].

Scheme 7

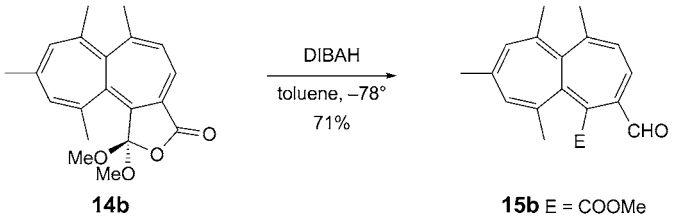

14b **15b** E = COOMe

Scheme 8

16b R^1 = H, R^2 = ^{i}Pr; 71% (3 h)[a]) R^1 = Me, R^2 = H; 75% (6 h) **17b**

[a]) Results taken from [2]. E = COOMe

When we subjected the mixture **4a**/**4b** to our former conditions at 80°[5]), we observed only the formation of 1-[(1*E*)-2-(dimethylamino)ethenyl]-5,6,8,10-tetramethylheptalene-2-carboxaldehyde (**18a**; *Scheme 9*). Most of the starting material, enriched in **4b**, was recovered as a *ca.* 3:1 mixture **4b**/**4a**. In the present case, MeO^- (formed by thermal dissociation of DMFDMA) was obviously not strong enough to deprotonate the remote Me–C(1) of **4b**, whereas Me–C(1) in vinylogous position of the CHO group of **4a** seems to be acidic enough for deprotonation.

Scheme 9

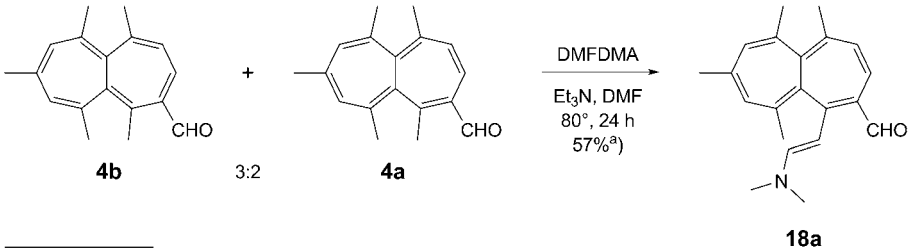

4b 3:2 **4a** **18a**

[a]) Yield with respect to reacted **4a**.

[5]) The DBS process **4a** ⇌ **4b** is extremely slow at the given temperature.

Indeed, when we subjected 4-formylheptalene-5-carboxylate **15b** to our (dimethylamino)ethenylation conditions, the correspondingly substituted product **19b** was isolated in acceptable yields[6]) (*Scheme 10*).

Scheme 10

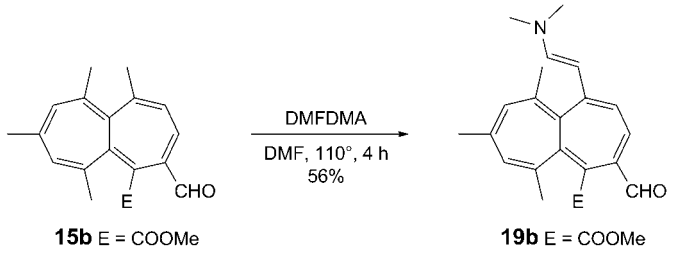

15b E = COOMe **19b** E = COOMe

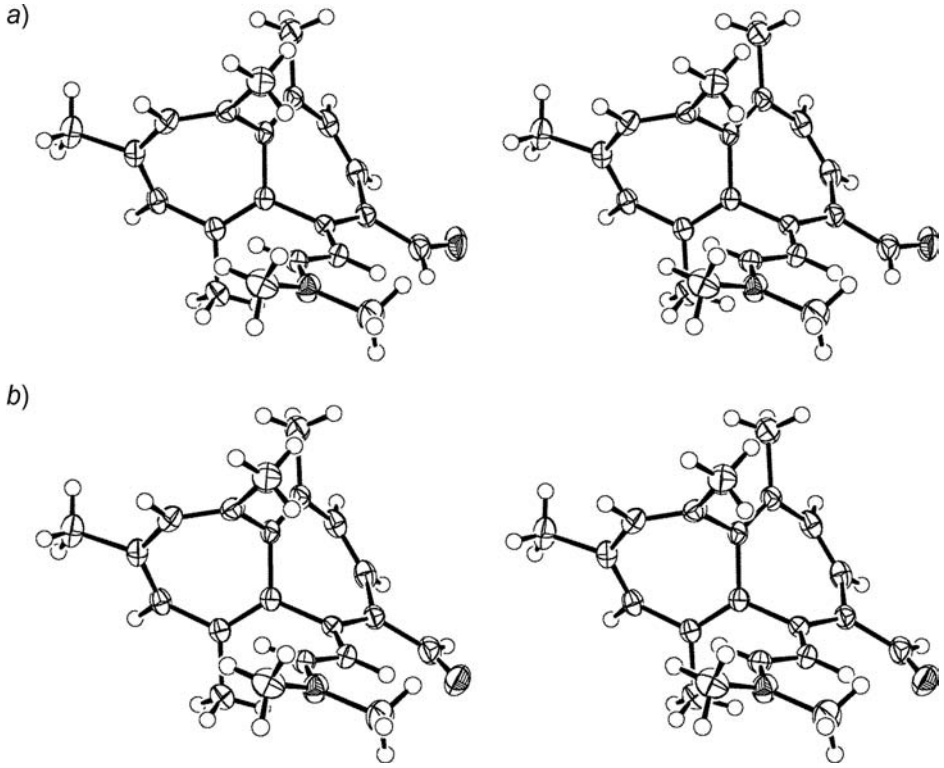

Fig. 3. *Stereoscopic view of the two conformations found in the crystals of 1-[(1*E*)-2-(dimethylamino)-ethenyl]-5,6,8,10-tetramethylheptalene-2-carboxaldehyde* (**18a**)

---

[6]) The corresponding aldehyde reactant with ^{i}Pr–C(9) instead of Me–C(8,10) gave only 10% of the 1-[(1*E*)-2-(dimethylamino)ethenyl]heptalene-4-carboxaldehyde analog of **19b** [2].

A wine-red prismatic crystal of **18a** was subjected to an X-ray crystal-structure analysis (*Fig. 3*). The analysis showed that **18a** appears in two conformations with respect to Θ(O=C–C(2)=C(1)) in the crystal lattice. The major conformation (*ca.* 77%; *Fig. 3*,*a*) displays a dihedral angle of 179.7(2)°, whereas in the minor form (*Fig. 3*,*b*) this angle amounts to −13.9(5)°. The minor conformation seems to be supported by weak intramolecular H-bonding ($d = 237$ pm) between the aldehyde O-atom and H–C(1′) of the ethenyl group at C(1). A similar nearest O ··· H contact ($d = 237$ pm) is also found in the major conformation between the O-atom of the aldehyde group and one of the H-atoms of the *anti*-oriented Me group of Me_2N–C(2′)=C(1′) of a neighboring molecule.

The fact that under our standard conditions, the reaction of **4b**/**4a** gave only the aminoethenylation product of **4a** (*Scheme 9*) led us to try the aminoethenylation reaction of **4b**/**4a** with *N*,*N*,*N*′,*N*′,*N*″,*N*″-hexamethylmethanetriamine (= tris(dimethylamino)methane = TDMAM), which would thermally dissociate to yield *N*-[(dimethylamino)methylene]-*N*-methylmethanaminium dimethylamide, so that the formed amide as the stronger base (as compared with MeO^-) may also deprotonate the less acidic Me–C(1) of **4b**. Indeed, the reaction of the **4b**/**4a** mixture in the presence of TDMAM gave almost equal amounts of the aminoethenylation products **18a** and **20b** (*Scheme 11*). The two products could be separated by CC (Al_2O_3). The dark red crystals of **20b**, dissolved in (D_6)acetone, showed $^3J(2,3) = 7.0$ Hz, which confirmed the position of the C–C and C=C bonds in heptalene **20b**.

Scheme 11

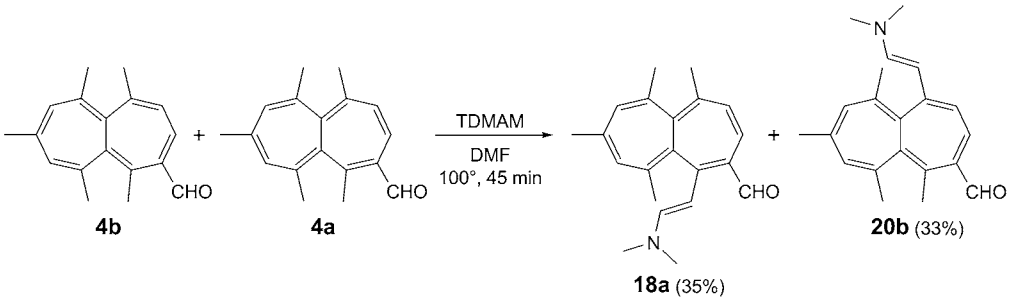

Since the condensation of the DBS mixture **4b**/**4a** with malononitrile (**1**) under *Knoevenagel* conditions gave the corresponding (heptalenylmethylene)malononitriles **21b** and **21a** only in a yield of 31%[7]), we searched for other condensation conditions

[7]) We found no indications for the formation of *Michael* adducts, *e.g.*, **22**, or follow-up products of it in these reactions as we had observed with heptalenedicarboxylates and sulfonylmethanides (see [15] and refs. cit. therein).

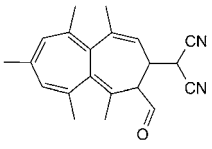

22

Scheme 12[a])[b])

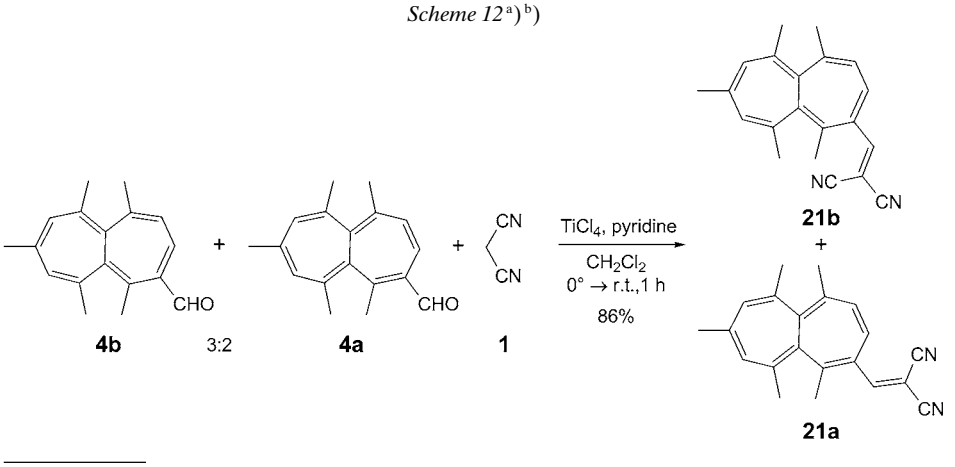

[a]) Piperidine (cat.), EtOH, reflux; 31% **21b**/**21a** (*cf.* [7]).

[b]) AcOH, $AcONH_4$, toluene, reflux; 0% **21b**/**21a** (*cf.* [17]).

and found that $TiCl_4$ and pyridine in CH_2Cl_2 [16] led to excellent yields of **21b**/**21a** (*Scheme 12*).

This procedure could also be applied to the 1-[(1*E*)-2-(dimethylamino)ethenyl]-heptalene-4-carboxaldehydes **19b** and **20b**, which furnished the corresponding (heptalen-4-ylmethylene)malononitriles **23b** and **24b**, respectively, in acceptable yields (*Scheme 13*). Both compounds were purified by CC (Al_2O_3) and finally crystallized from pentane/CH_2Cl_2 and hexane/Et_2O (for **23b** and **24b**, resp.). In this way, **23b** was obtained as green, metallically shiny needles and **24b** as green, metallically shiny prisms. The crystals of both heptalenic merocyanines dissolved easily in polar solvents with wine-red to blue color depending on the polarity of the solvent (see later).

Scheme 13

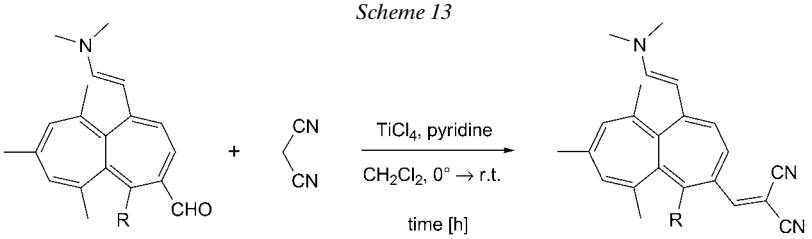

The X-ray crystal structure of both **23b** and **24b** showed some interesting features (*Figs. 4* and *5*; *Tables 1* and *2*). The 2-(dimethylamino)ethenyl group at C(1) occupies in both compounds an almost perfect s-*trans* orientation at C(1′)–C(1). However, the orientation of the 2,2-dicyanoethenyl group at C(4) of the two molecules is different. Whereas **23b** displays in the crystal at C(1″)–C(4) an s-*cis* arrangement, it is s-*trans* in

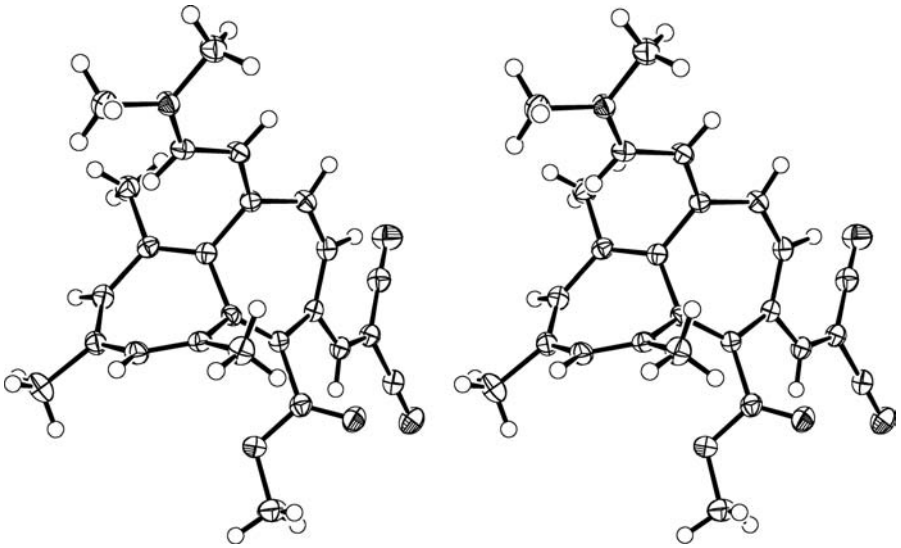

Fig. 4. *Stereoscopic view of the X-ray crystal structure of methyl 4-(2,2-dicyanoethenyl)-1-[(1*E*)-2-(dimethylamino)ethenyl]-6,8,10-trimethylheptalene-5-carboxylate* (**23b**)

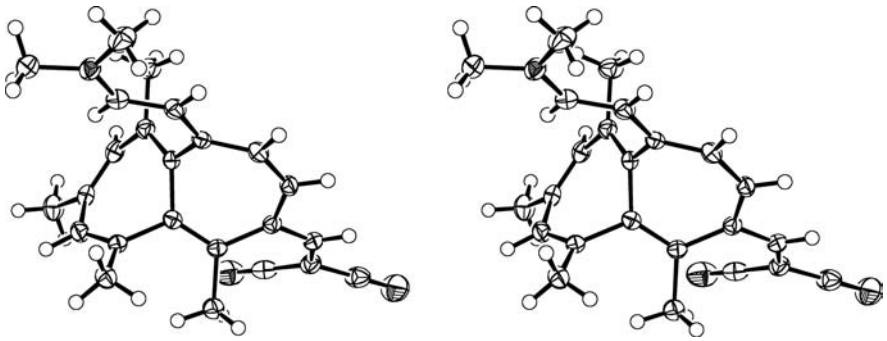

Fig. 5. *Stereoscopic view of the X-ray crystal structure of 2-{{[(1*E*)-2-(dimethylamino)ethenyl]-5,6,8,10-tetramethylheptalen-4-yl}methylene}malononitrile* (**24b**)

the crystal of **24b** (*Table 2*). Obviously the space at $(NC)_2C{=}CH{-}C(4)$ and MeOOC–C(5) is too tight for an s-*trans* arrangement of the 2,2-dicyanoethenyl group in relation to C(3)=C(4) of the heptalene part. As a further consequence, the ester C=O group of **23b** is turned almost out of conjugation (*cf.* Θ(C(5a)=C(5)–C=O); *Table 2*).

The strong electronic interaction of the 2-(dimethylamino)ethenyl group at C(1) and the 2,2-dicyanoethenyl substituent at C(4) across the heptalene bonds C(1) to C(4) is documented by almost equal bond lengths in the narrow range of 140.5 – 138.6 pm of the merocyanine part of **23b** and **24b**, in contrast to 1,3,5,6,8,10-hexamethylheptalene (**25**) as typical heptalene with alternating C–C and C=C bonds in its core (*cf. Table 1*).

Table 1. *Selected Bond Lengths of* **23b** *and* **24b** *in Comparison with Those of* **25**[a])

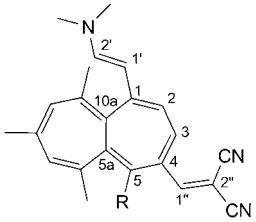

	Bond length *d* [pm]		
	23b (R = COOMe)	**24b** (R = Me)	**25**
C(1)–C(2)	140.2(2)	139.3(2)	134.4(2)
C(2)–C(3)	138.6(2)	138.7(2)	146.0(2)
C(3)–C(4)	139.7(2)	140.5(2)	135.4(2)
C(4)–C(5)	147.2(2)	148.1(2)	145.5(2)
C(5)–C(5a)	135.1(2)	134.6(2)	135.1(2)
C(1)–C(10a)	148.9(2)	149.0(2)	149.4(2)
C(1)–C(1′)	139.9(2)	140.6(2)	–
C(1′)–C(2′)	138.6(2)	138.0(2)	–
C(4)–C(1″)	141.8(2)	141.2(2)	–
C(1″)–C(2″)	138.4(2)	138.0(2)	–
N–C(2′)	132.2(2)	133.2(2)	–

[a]) 1,3,5,6,8,10-Hexamethylheptalene (**25**) [11].

Table 2. *Size of Torsion Angles of* **23b** *and* **24b** *in Comparison with Those of* **25**[a])

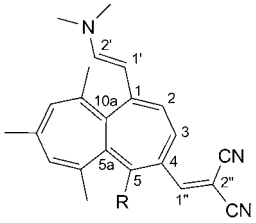

	Torsion angle Θ [°]		
	23b (R = COOMe)	**24b** (R = Me)	**25**
C(1)=C(2)–C(3)=C(4)	19.4(3)	16.8(2)	31.1(3)
C(3)=C(4)–C(5)=C(5a)	34.2(2)	35.2(2)	31.3(3)
C(5)=C(5a)–C(10a)–C(1)	67.3(2)	69.2(2)	62.9(2)
C(6)=C(5a)–C(10a)–C(10)	69.3(2)	68.5(2)	62.9(2)
C(6)=C(7)–C(8)=C(9)	34.2(2)	34.6(2)	35.4(3)
C(8)=C(9)–C(10)=C(10a)	31.6(2)	34.6(2)	33.1(3)
C(2)=C(1)–C(1′)=C(2′)	178.9(1)	172.4(1)	–
C(3)=C(4)–C(1″)=C(2″)	13.1(3)	159.1(1)	–
C(5a)=C(5)–C=O	127.2(2)	177.6(1)[b])	173.5(2)[b])
N–C(2′)=C(1′)–C(1)	175.5(1)	179.2(1)	–

[a]) 1,3,5,6,8,10-Hexamethylheptalene (**25**) [11]. [b]) C(10a)–C(5a)=C(5)–Me.

Distinctly flattened is also the torsion angle at C(2)–C(3), a fact that leads to a stronger torsion at the central σ-bond C(5a)–C(10a) as indicated by the corresponding *cisoid* angles of **23b** and **24b** (69.3 – 67.3°) in comparison with that of **25** (62.9°) with pseudo C_2 symmetry in the crystals. The structure of **23b** and **24b** is therefore defined by a strong contribution of their corresponding zwitterionic forms (*Fig. 6*). This fact is also underlined by the size of ^3J(H–C(2),H–C(3)) = 7.6 and 7.9 Hz, respectively, of the two compounds, which is far beyond ^3J(H–C(2),H–C(3)) = 5.7 Hz of **15b** (*Scheme 7*), the precursor of **23b** and a typical prototype of heptalenes with fully substituted *peri*-positions[8]).

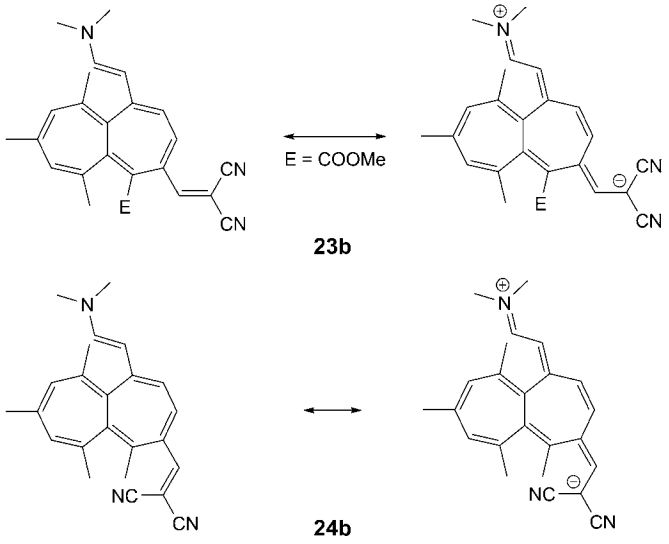

Fig. 6. *Charge distribution of* **23b** *and* **24b**

The reaction of the 1-[(1*E*)-2-(dimethylamino)ethenyl]heptalene-2-carboxaldehyde **18a** under our standard conditions with malononitrile took place only sluggishly and resulted in the formation the expected (2,2-dicyanoethenyl)heptalene **26a** solely in moderate yields (*Scheme 14*,*a*). An unexpected product **27** was isolated in slightly higher yield. Both products differed scarcely from each other in view of their analytical and spectroscopic behavior. Both compounds were obtained as violet powders, which after crystallization from pentane/CH_2Cl_2 formed green metallically shiny needles with almost identical melting points. Their IR, ^{1}H-NMR, and mass spectra did not provide data for a secure identification. Nevertheless, their slight difference in polarity was sufficient to separate them by CC (silica gel). The less polar **26a** was thus obtained in wine-red fractions, followed by violet fractions of **27**. The structure of both products was finally solved by X-ray crystal-structure analyses (*Figs. 7* and *8*). Most interesting was the aspect that **26a** could principally also exist in its DBS form **26b**, whereas **27** represented a lock-in heptalene structure with a high zwitterionic component (*Scheme 14*,*b*).

---

[8]) The average ^3J(H,H) value for this type of heptalenes amounts to 6.0 ± 0.3 Hz.

Scheme 14

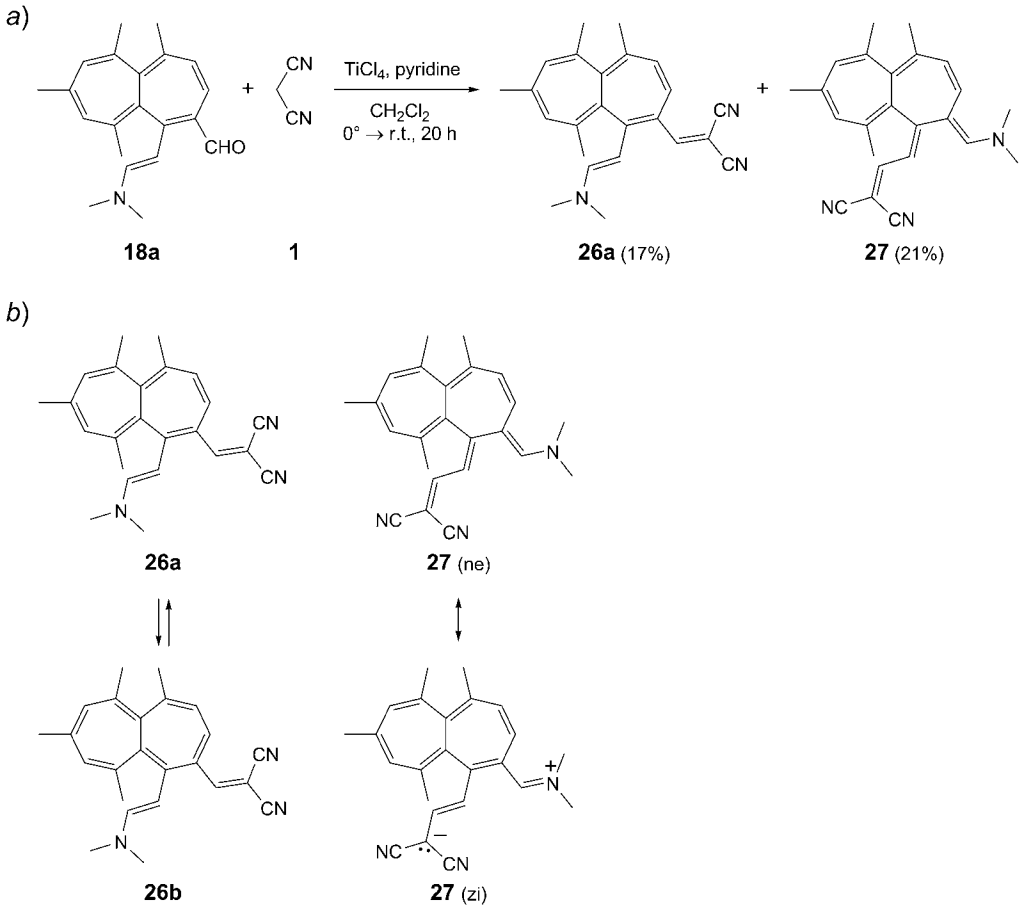

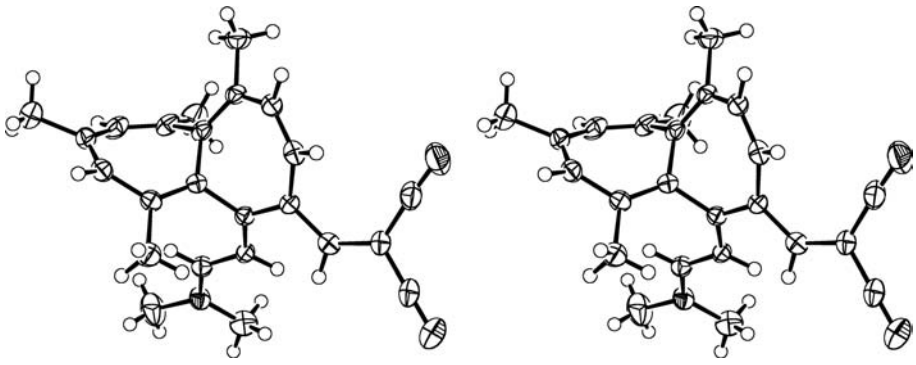

Fig. 7. *Stereoscopic view of the X-ray crystal structure of 2-{[1-[(1*E*)-2-(dimethylamino)ethenyl]-5,6,8,10-tetramethylheptalen-2-yl]methylene}malononitrile* (**26a**)

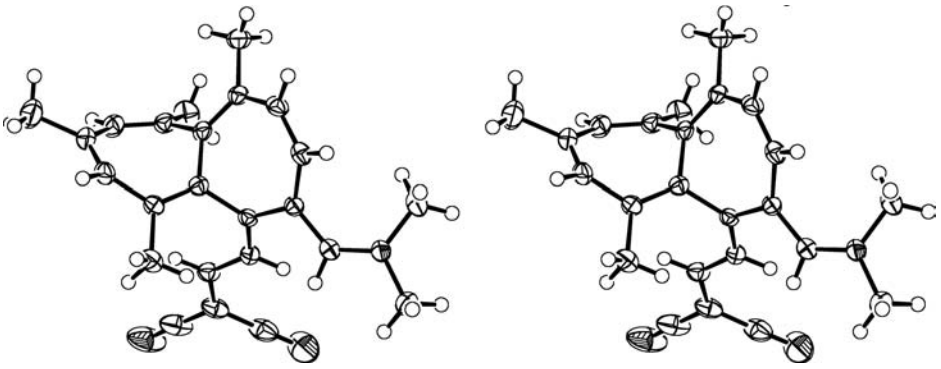

Fig. 8. *Stereoscopic view of the X-ray crystal structure of 2-{{2*E*)-2-{(2*E*)-2-[(dimethylamino)methylene]-5,6,8,10-tetramethylheptalen-1(2*H*)-ylidene}ethylidene}malononitrile* (**27**)

The structure analysis of both heptalene-1,2-diyl merocyanines **26b** and **27** revealed again a high degree of bond delocalization if one takes for both compounds *d*(C(3)=C4)) and *d*(C(4)–C(5)) as reference for the length of C–C and C=C bonds in heptalene skeletons (*cf. Table 3*). The lengths of C(1),C(2) of **26a** and **27** are more or less identical and show an average length close to the middle of typical C–C and C=C

Table 3. *Selected Bond Lengths of* **26a** *and* **27**

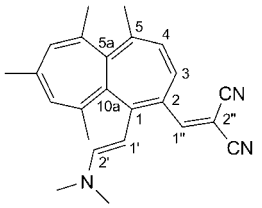

26a

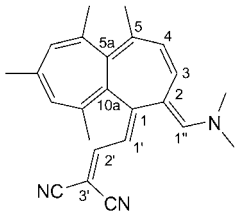

27

	Bond length [pm]	
	26a	**27**
C(1)–C(2)	141.9(3)	142.8(2)
C(2)–C(3)	145.6(3)	145.2(2)
C(3)–C(4)	134.4(3)	134.8(2)
C(4)–C(5)	145.3(3)	145.0(2)
C(5)–C(5a)	135.1(3)	135.0(2)
C(1)–C(10a)	149.1(3)	149.1(2)
C(1)–C(1′)	140.1(3)	139.0(2)
C(1′)–C(2′)	137.8(3)	138.9(2)
C(2)–C(1″)	141.0(3)	140.5(2)
C(1″)–C(2″)	138.1(3)	138.0(2)
C(5a)–C(10a)	147.9(3)	148.0(2)
N–C(1″)	131.9(3)	132.4(2)
C(2′)–C(3′)	–	139.1(2)

bonds of heptalenes with substituents at all four *peri*-positions. The presence of 'one and a half' bond between C(1) and C(2), especially in **26a**, is also indicated by the *exo*-torsion angle of 24.1° at this bond (*cf. Table 4*). Its structural isomer **27** exhibits for the analog fragment a Θ value of 30.2°, only slightly lower than the *endo*-torsion angle at C(4) and C(5) of **27** ($\Theta = 31.6°$), which can be regarded as typical for heptalenes with substituents at all four *peri*-positions[9]).

Table 4. *Size of Torsion Angles of* **26a** *and* **27**

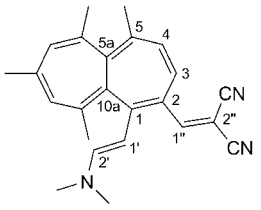

26a

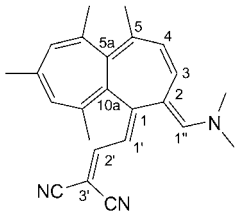

27

	Torsion angle Θ [°]	
	26a	**27**
C(1)=C(2)–C(3)=C(4)	27.2(4)	21.9(2)
C(3)=C(4)–C(5)=C(5a)	31.5(2)	31.6(2)
C(5)=C(5a)–C(10a)–C(1)	67.3(4)	62.5(2)
C(6)=C(5a)–C(10a)–C(10)	65.5(3)	63.8(2)
C(6)=C(7)–C(8)=C(9)	33.0(4)	34.1(3)
C(2)=C(1)–C(1′)=C(2′)	174.1(2)	179.6(1)[a])
C(1)=C(2)–C(1″)=C(2″)	171.6(2)	166.5(1)[b])
C(1′)–C(1)=C(2)–C(1″)	24.1(3)	30.2(2)[c])
C(1″)–C(2)=C(3)–C(4)	156.1(2)	165.2(1)
N–C(2′)=C(1′)–C(1)	178.3(2)	–

[a]) C(2)=C(1)–C(2′)=C(3′). [b]) N–C(1″)=C(2)–C(1). [c]) C(1′)=C(1)–C(2)=C(1″).

A plausible mechanism for the formation of **26b** and **27** involves the conformers s-*trans*-and s-*cis*-**18a** (conformer with respect to the C(1)–C(1′) bond; *Scheme 15*). Thus, **26b** would be formed *via* **I** (1) from s-*trans*-**18a**, and **27** from s-*cis*-**18a** *via* s-*trans*-**I** (2), s-*cis*-**I** (2), and **I** (3).

2.3. *Example of a New Entrance to Symmetrically 1,4-Di-π-substituted Heptalenes.* The formation of the 4-(hydroxymethyl)heptalene-1-carboxaldehyde **13b** (*Scheme 5*) led to the question how this heptalene with functional groups in 1,4-relation could be implemented in an easy synthesis of 1,4-di-π-substituted heptalenes as described in the foregoing publication [1]. Therefore, we investigated the selective oxidation of the CH_2OH group of **13b** to an CHO group. We realized the best results with 4-methylmorpholine 4-oxide monohydrate (NMO) in the presence of tetrapropylam-

[9]) The corresponding AM1-calculated torsion angles of C_2 symmetric 1,5,6,10-tetramethylheptalene amount to 32°.

Scheme 15

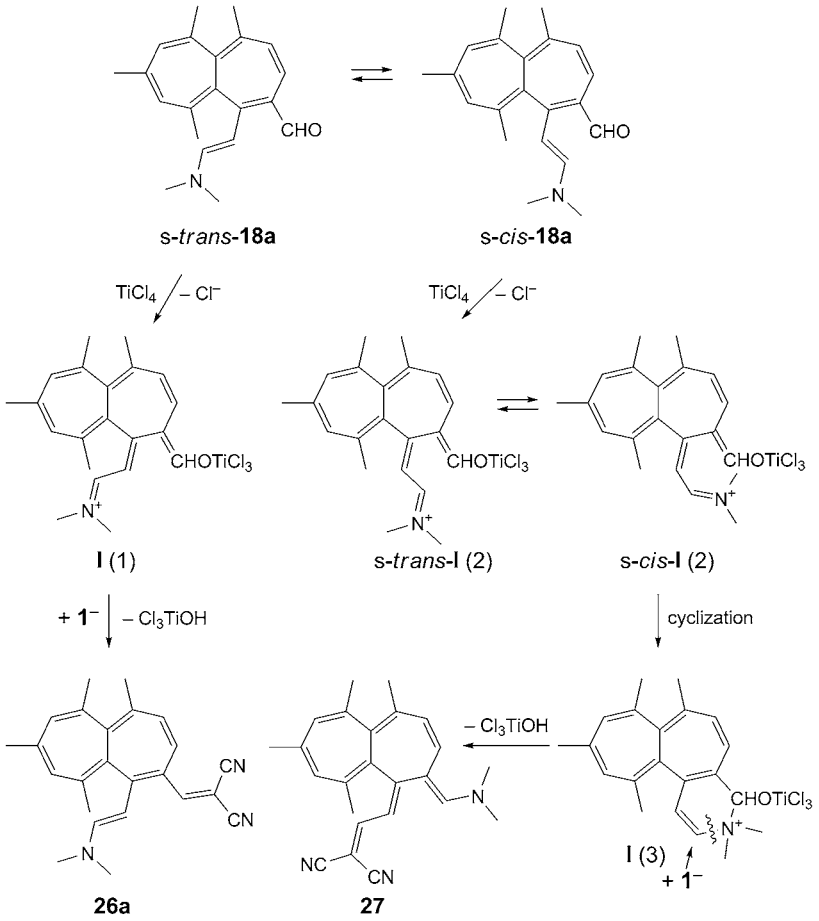

monium perruthenate (TPAP) (*cf.* [18]) in CH_2Cl_2. Dicarboxaldehyde **28b** and its DBS isomer **28a** were thus obtained in a total yield of 70% (*Scheme 16*). The *Swern* oxidation of **13b** with DMSO/$(COCl)_2$ gave the two dicarboxaldehydes in a 1:1 ratio and a total yield of only 47%. In later experiments, we found that pure **28b** is accessible in nearly quantitative yield by oxidative cleavage of the enamine bond of **19b** with $NaIO_4$ in aqueous THF (*Scheme 16*; *cf.* [19]). This procedure was not applicable to the synthesis of heptalene-1,2-dicarboxaldehyde **29a** by cleavage of the enamine bond of **18a** (*Scheme 16*), since **18a** decomposed completely in the course of its oxidative cleavage.

We were not able to separate chromatographically the mixture **28b**/**28a**, which gave on crystallization an orange crystal powder made of the red crystals of **28b** (72%) and the yellow crystals of **28a** (28%). Both compounds were clearly distinguishable by their ^{1}H-NMR spectra in $CDCl_3$ with $^3J(2,3) = 6.0$ Hz for **28b** and 12.0 Hz for **28a**, respectively, and, as expected, the *s* signals for the H-atom of the CHO groups

Scheme 16

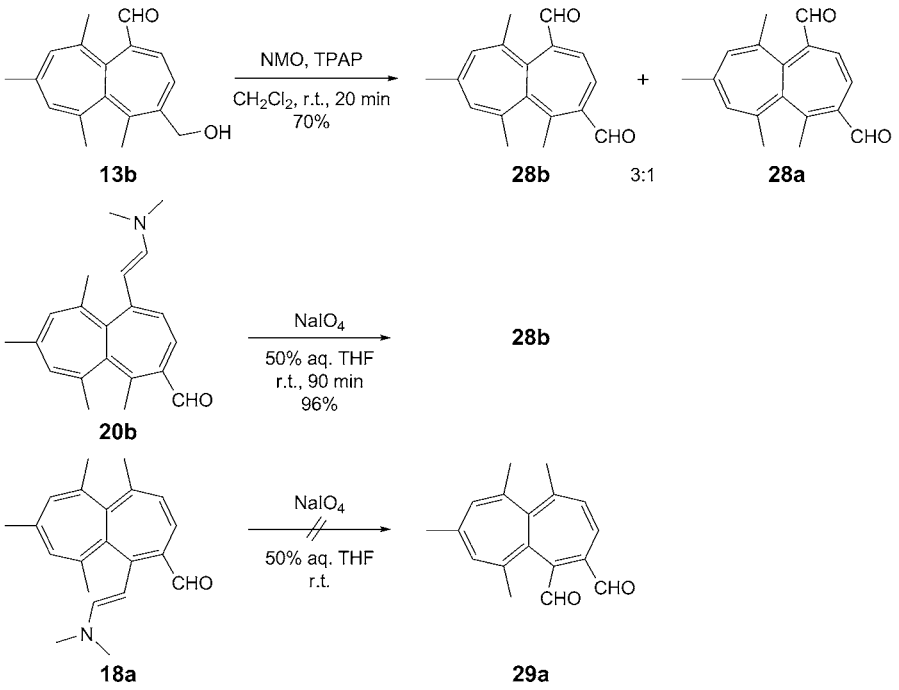

appeared at lower field for **28a** (2 *s* at δ(H) 10.18 and 9.87) than for **28b** (2 *s* at δ(H) 9.73 and 9.61). Finally, we got a red crystal of **28b** suitable for an X-ray diffraction analysis, which established unequivocally the structure of **28b** with no unusable feature (*Fig. 9*). Both aldehyde C=O groups show with their respective C=C bonds a nearly perfect s-*trans* arrangement with torsion angles of 170.3(2)° (C(1)=C(2)) and 162.1(2)° (C(4)=C(3)).

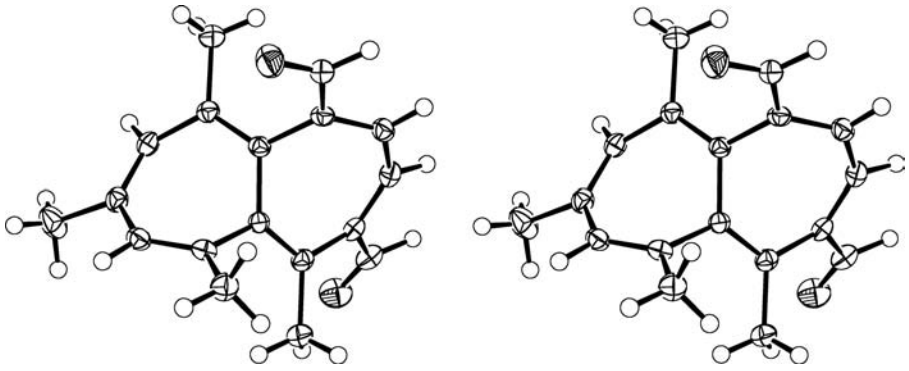

Fig. 9. *Stereoscopic view of the X-ray crystal structure of 5,6,8,10-tetramethylheptalene-1,4-dicarboxaldehyde* (**28b**)

With the pure heptalene-1,4-dicarboxaldehyde **28b** in hands, we tested its utility in a double *Horner–Wittig* reaction with diethyl *P*-cinnamylphosphonate [20] (*Scheme 17*). The reaction worked principally and delivered the desired 5,6,8,10-tetramethyl-1,4-bis[(1*E*,3*E*)-4-phenylbuta-1,3-dien-1-yl]heptalene (**30b**) as main product, however, accompanied by two by-products, which we supposed to be the 'mono-products' **31b** and **32b** (*Scheme 17*). Unfortunately, we could not separate the products by chromatography. Moreover, it seemed that **30b** was much more sensitive than its analog where Me–C(5) is exchanged by MeOOC–C(5) and which we had investigated in more detail [1].

Scheme 17

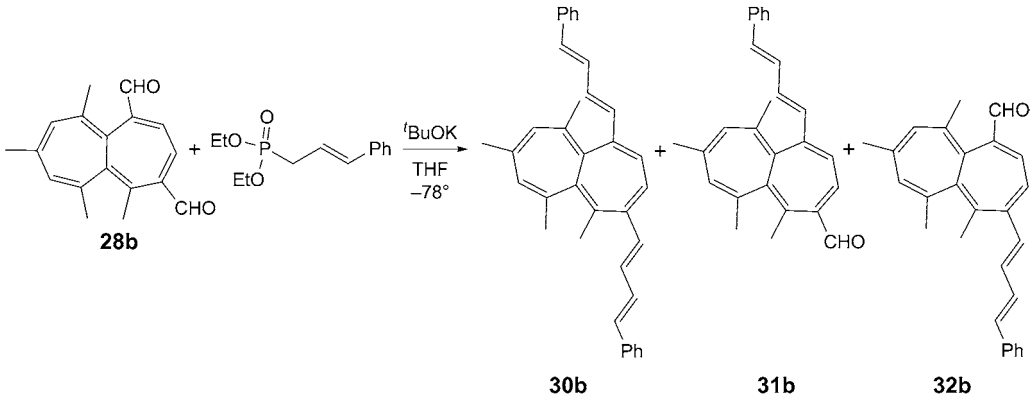

2.4. *UV/VIS Behavior of the New Heptalene-Based Merocyanines.* 2.4.1. *Preamble.* We showed already in our former publications that the longest-wavelength-absorption band of 1,4-di-π-substituted heptalenes (heptalene band I [12]) carries strong charge-transfer (CT) character like their comparable open-chain analogs and that it makes the largest contribution to the absorption in total above 200 nm of these heptalenes (see [1][2]). This behavior is still more pronounced for the heptalenes of this work, which includes the 1,2-di-π-substituted heptalenes **26a** and **27**.

2.4.2. *1,4-Di-π-substituted Heptalenes.* The UV/VIS spectra of the heptalenecarboxaldehydes and their corresponding 2,2-dicyanoethenyl derivatives **20b** and **24b**, and **19b** and **23b** in MeCN are displayed in *Figs. 10* and *11*, and *Figs. 12* and *13*, respectively. They reflect the influence of the electronic nature of the substituent at C(5) (COOMe as π-acceptor in **19b** and **20b** *vs.* Me as σ-donor in **23b** and **24b**). The λ_{max} (log ε) values of band I and II of the four donor-acceptor substituted heptalenes are listed in *Table 5*. The CT band of the two aldehydes **19b** and **20b** appears at distinctly longer wavelength than that of open-chain (all-*E*)-7-(dimethylamino)hepta-2,4,6-trienal (420 nm ($CHCl_3$), 418 nm (MeCN) [21]). The same is true for the CT band of the two malononitrile derivatives and its open chain analog 2-((all-*E*)-7-(dimethylamino)-hepta-2,4,6-trien-1-ylidene)malononitrile (550 nm ($CHCl_3$) [4]). These tendencies are much less expressed by heptalenes with less polarizing phenyl capped (1*E*)-ethenyl and (1*E*,3*E*)-buta-1,3-dien-1-yl groups in 1,4-position [1]. As a result, it can be said that the

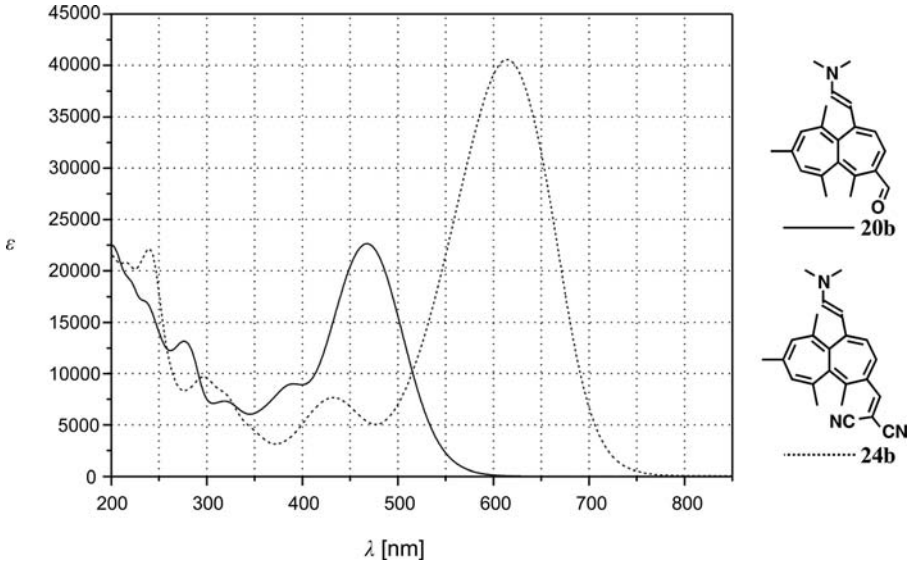

Fig. 10. *UV/VIS Spectra of* **20b** *and* **24b** *in MeCN*

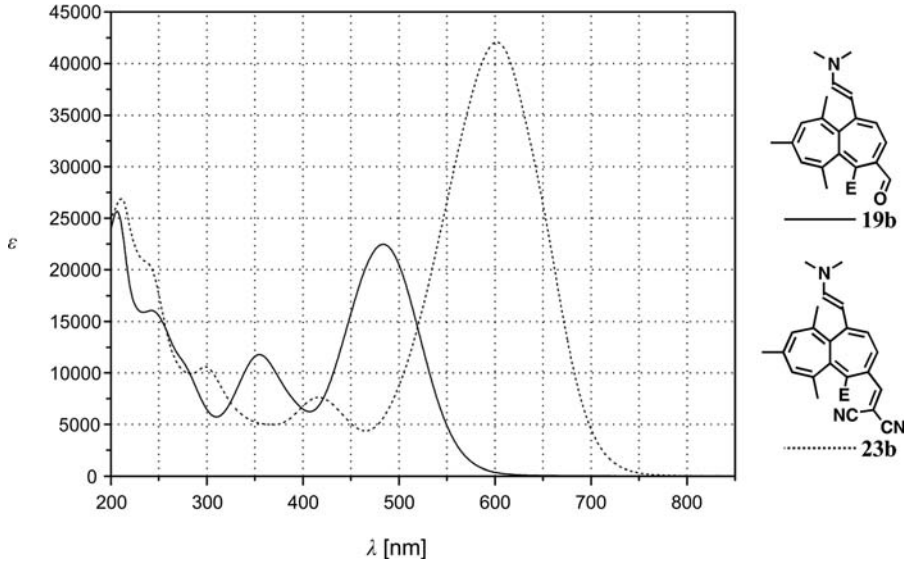

Fig. 11. *UV/VIS Spectra of* **19b** *and* **23b** *in MeCN*. E = COOMe.

stronger the polarization of the merocyanine part of the heptalenes is, the more electron density is contributed from the residual 7-methylenecyclohepta-1,3,5-triene part of the heptalene core to the merocyanine entity leading thus to a bathochromic shift of the CT band as compared with the corresponding open-chain linear forms. There is another indicator which supports this observation. The CT band of

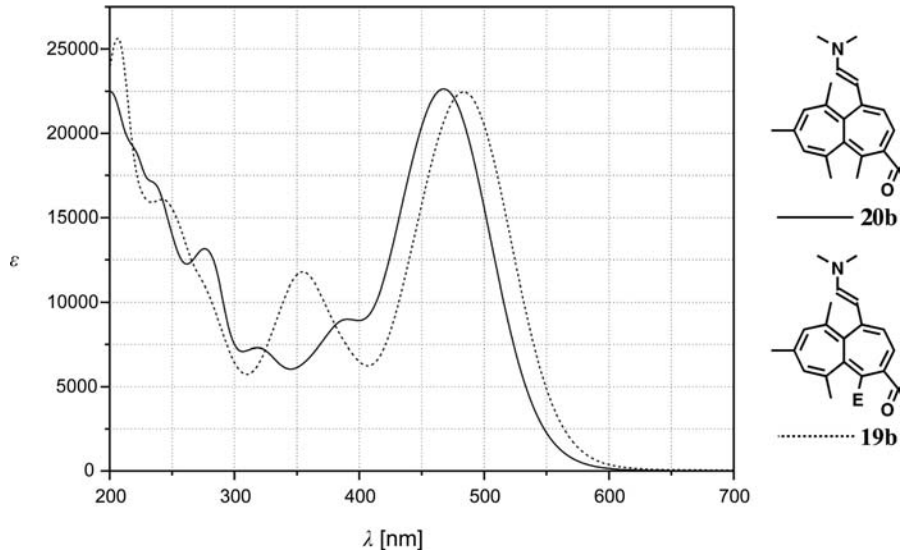

Fig. 12. *UV/VIS Spectra of* **19b** *and* **20b** *in MeCN.* E = COOMe.

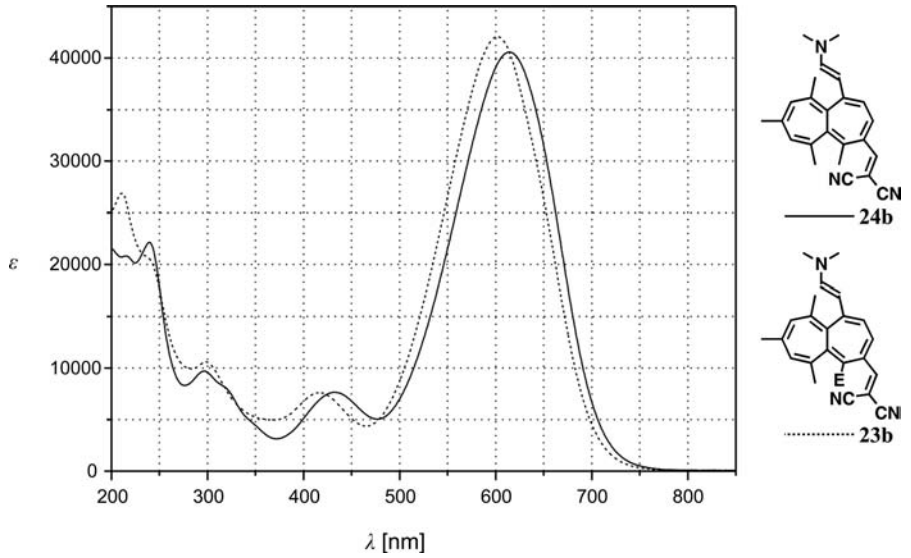

Fig. 13. *UV/VIS spectra of* **23b** *and* **24b** *in MeCN.* E = COOMe.

carboxaldehyde **19b** with MeOOC–C(5) is in comparison to carboxaldehyde **20b** with Me–C(5) bathochromically shifted by 17 nm, in contrast to their malononitrile derivatives **23b** and **24b** where one observes a hypsochromic shift of 12 nm (*Table 5*; *Figs. 12* and *13*). Obviously the 2-(cyclohepta-2,4,6-trien-1-ylidene)acetate (= 8-(methoxycarbonyl)heptafulvene) part of **19b** takes some electron density from the

Table 5. *Position of Heptalene Band I* (CT) *and II of Aldehydes* **19b** *and* **20b** *and Their Malononitrile Derivatives* **23b** *and* **24b**[a])

	Band I λ [nm] (log ε)	Band II λ [nm] (log ε)	$\Delta\lambda$(I)[b]) [nm]	$\Delta\lambda$(II)[b]) [nm]
19b	484 (4.35)	355 (4.07)		
23b	602 (4.62)	416 (3.88)	118	61
20b	467 (4.35)	391 (3.95)		
24b	614 (4.61)	432 (3.88)	147	41

[a]) In MeCN. [b]) $\Delta\lambda$ (malononitrile derivative – aldehyde).

merocyanine part and thus enhances the polar character in total of the molecule, whereas an opposite effect is working in **20b** with its 7-ethylidenecyclohepta-1,3,5-triene (= 8-methylheptafulvene) part. These subtle electronic effects are outmaneuvered by the much stronger π-acceptor quality of the 2,2-dicyanoethenyl groups of **23b** and **24b**. The above considerations are supported by a distinct larger extinction coefficient of the heptalene band II of **19b** in comparison to **20b** (*Table 5*; *Fig. 12*). In the case of **23b** and **24b** (*Table 5*; *Fig. 13*), the heptalene band II are of equal intensity.

2.4.3. *1,2-Di-π-substituted Heptalenes.* The UV/VIS spectra of the new heptalenes **18a** and **26a** with the donor and acceptor substituent in a 1,2-relation are displayed in *Fig. 14*, and the corresponding λ (log ε) values are listed in *Table 6*. Both heptalenes exhibit in comparison with their open-chain analogs, (all-*E*)-5-(dimethylamino)penta-2,4-dienal (λ_{max} ($CHCl_3$) 363 nm [21b]) and (all-*E*)-5-(dimethylamino)penta-2,4-dien-1-ylidene)malononitrile (λ_{max} ($CHCl_3$) 478 nm [4]), strong bathochromic shifts of $\Delta\lambda = +86$ nm (**18a**) and $\Delta\lambda = +66$ nm (**26a**), respectively[10]). Most interesting is that the λ_{max} value of **27** with a comparable bond length and *exo*-torsion angle at C(1),C(2) to those of **26a** (*Table 4*) shows, with respect to its open-chain analog, a still stronger bathochromic shift of $\Delta\lambda = +80$ nm. On the other hand, as already mentioned, compound **27** represents a special heptalene based merocyanine with structurally locked π-bonds, which means that the cyclic DBS process is not possible in this case (*Scheme 14*,*b*).

Table 6. *Position of Heptalene Band I* (CT) *and II of Aldehyde* **18a** *and Its Malononitrile Derivatives* **26a** *and* **27**[a])

	Band I λ [nm] (log ε)	Band II λ [nm] (log ε)	$\Delta\lambda$(I)[b]) [nm]	$\Delta\lambda$(II)[b]) [nm]
18a	449 (4.17)	358 (4.03)		
26a	544 (4.53)	396 (3.99)	95	38
27	558 (4.50)	394 (4.03)		

[a]) In MeCN. [b]) $\Delta\lambda$ (malononitrile derivative – aldehyde).

[10]) Merocyanines of the discussed type show almost no differences of their λ_{max} values in $CHCl_3$ and MeCN [21a].

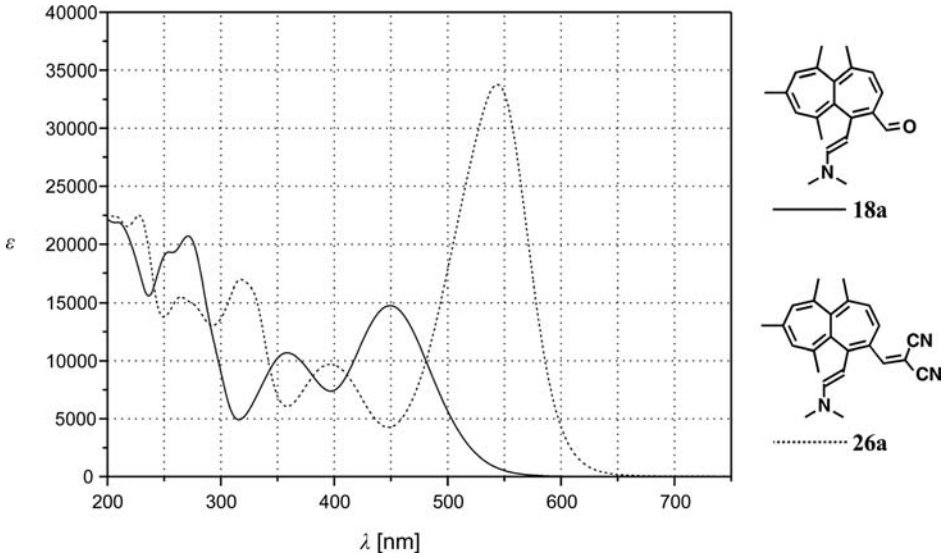

Fig. 14. *UV/VIS Spectra of* **18a** *and* **26a** *in MeCN*

2.5. *Photochromic Behavior of the New Heptalene-Based Merocyanines.* 2.5.1. *Preamble.* In *Table 7* is listed the solvent dependence of the position of the CT band of heptalene-based merocyanines of this work together with one of a former work, amounting in average to *ca.* +40 nm in going from MeCN to cyclohexane or hexane, respectively. Most extreme deviations from the average value are observed for **18b** ($\Delta\lambda + 9$ nm) with the smallest degree of polarization and for **23b** ($\Delta\lambda + 91$ nm) with the highest degree of polarization. It was therefore of interest for us to study the photochemical behavior of the new merocyanines in MeCN as strong supporter of their zwitterionic character and in some cases in cyclohexane as non-stabilizing solvent of charge separation. Since all heptalenes showed a massively enhanced heptalene band I with expressed CT character, we performed all irradiations with a tungsten lamp (150 W) with its broad emission spectrum between 400–800 nm. For the study of the

Table 7. *Solvent Dependence of the Position of Heptalene Band I* (CT) *of Some Heptalene-Based Merocyanines*

	λ_{max} [nm]		$\Delta\lambda_{max}$ [nm]
	MeCN	cyclohexane	
19b	484	442	42
20b	467	434	33
23b	602	511	91
18a	449	440	9
26a	544	503	41
17b[a])	468	431[b])	37

[a]) *Scheme 8*, $R^1 = Me$, $R^2 = H$ [2]. [b]) Hexane.

thermal back reactions, the photo-equilibrated heptalene solutions were left in the dark at room temperature ($22 \pm 1°$). The start and changes in the spectra were measured at given time intervals. The development of the spectra of the photo-equilibrated mixtures at room temperature was registered in the same way without awaiting the thermal equilibrium state due to the slowness of the thermal back reaction at room temperature.

The carrying out of the individual experiments was simple: At first, a degassed solution of the corresponding heptalene compound was prepared under exclusion of light in the usual concentration for UV/VIS measurements of *ca.* $4 \cdot 10^{-5}$ M. The standard quartz cuvette with the prepared solution was then introduced in the UV/VIS spectrometer to measure the absorption spectrum. After this first measurement, the cuvette was placed at a distance of 10 cm with respect to the tungsten lamp and irradiated for a certain time interval (Δt). This procedure was repeated until no further changes of the absorption spectrum were observed indicating thus the photostationary state of the DBS process. This solution was then kept in the dark at room temperature and its UV/VIS spectrum measured again in larger time intervals to identify the onset of the thermal back reaction of the system.

2.5.2. *1,4-Donor–Acceptor Substituted Heptalenes.* In *Fig. 15*, the change of the spectrum of **19b** in MeCN on irradiation with time intervals of 20 s is shown. The exposure to white light leads to a strong hypochromic effect of the CT band of **19b**, whereas heptalene bands II, III, and IV increase (as indicated by the down- and upward showing arrows). The photostationary state between **19b** and **19a** is reached after 4 min accompanied by a reduction of the CT band to 23% of its original value. The clean reversible transformation of **19b** into its DBS isomer **19a** is clearly indicated by isosbestic points at 361, 222, and 204 nm.

When the MeCN solution, after reaching the photostationary state, is stored in the dark, the intensities the heptalene bands of **19b** grow again (*Fig. 16*), with the result

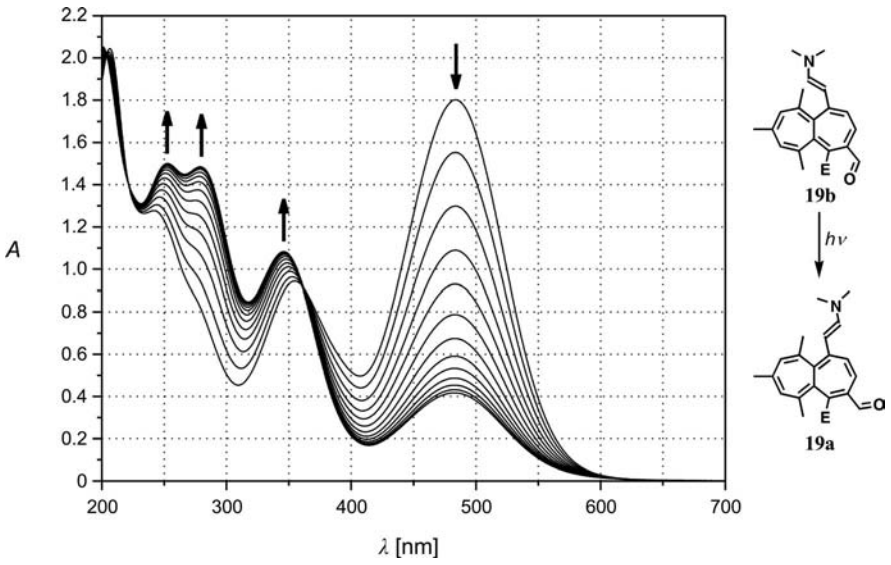

Fig. 15. *UV/VIS Spectra of the photoisomerization* **19b** → **19a** *in MeCN* ($\Delta t = 20$ s). E = COOMe.

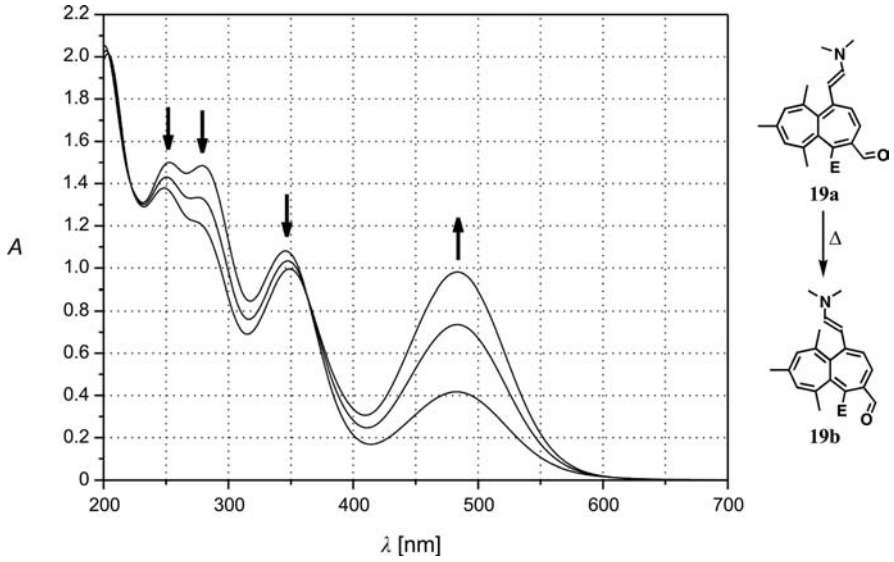

Fig. 16. *UV/VIS Spectra of the thermoisomerization* **19b** → **19a** *in MeCN* (r.t., $\Delta t = 1$ h). E = COOMe.

that after 2 h, the CT band has gained again already 54% of its original value of pure **19b**. This means that, without knowing the exact value, **19b** must distinctly predominate in the thermal equilibrium of **19b** and **19a**. This observation is in agreement with our former experiments which showed that on heating dimethyl 1-(2-[(1*E*)-dialkylamino)ethenyl]-9-isopropyl-6-methylheptalene-4,5-dicarboxylates (alkyl = Me, $-(CH_2)_n-$ ($n = 3-5$), $-(CH_2)_4O-$)[11]) on heating formed less than 1% of their DBS isomers. The fact that photochemically generated **19a** in MeCN undergoes the back reaction to **19b** slowly already at room temperature indicates a quite large difference in the ΔH_f^0 values of both DBS isomers combined with a comparably low activation energy (E_a) of the DBS process **19a** → **19b**.

In the described way, the photochemical transformation of all investigated merocyanines of the **B**-type could be observed, however, with individual differences due to their alteration in structure. This fact is already recognizable in the case of **20b**, the Me–C(5) analog of **19b**. The photostationary equilibrium **20b** ⇌ **20a** is reached within 2 min, whereby heptalene band I is reduced by 93% (*Fig. 17*) accompanied by a distinct growth of heptalene bands II and III. Isosbestic points are found at 370, 226, and 203 nm. Most interesting is the finding that the thermal back reaction at room temperature takes place very sluggishly in this case (*Fig. 18*). Responsible for this behavior is the steric interaction of Me–C(1) and Me–C(10) of **20a** in the transition state of the thermal DBS process leading to a higher E_a value in comparison to **19a**.

A surprise offered the investigation of **23b**, the malononitrile derivative of **19b**, under the standard irradiation conditions. Whereas the latter reaches the photostationary state after 4 min with a reduction of heptalene band I by 77% (*Fig. 15*), the

[11]) See Table 1 and text in [2].

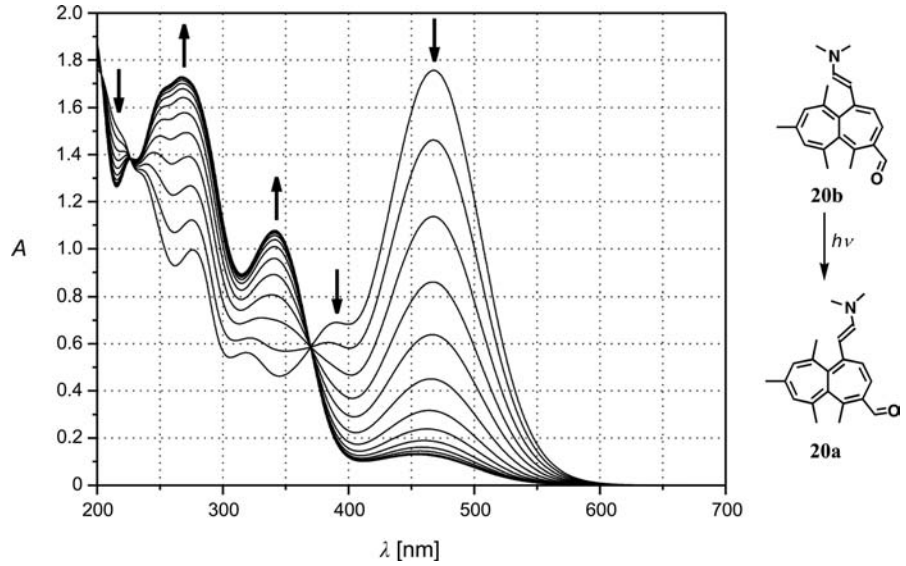

Fig. 17. *UV/VIS Spectra of the photoisomerization* **20b** → **20a** *in MeCN* ($\Delta t = 10$ s)

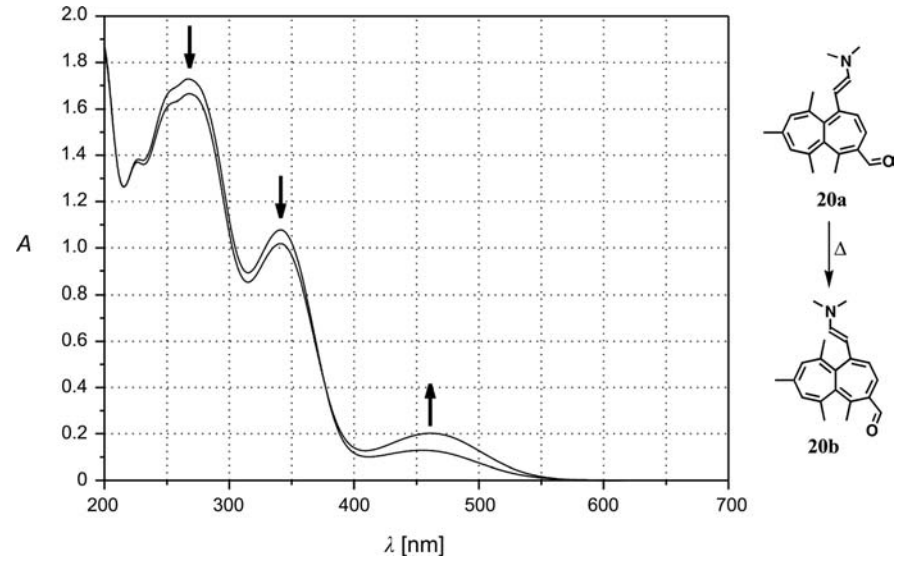

Fig. 18. *UV/VIS Spectra of the thermoisomerization* **20a** → **20b** *in MeCN* (r.t., $\Delta t = 24$ h)

process **23b** ⇌ **23a** leads only to a 19% reduction of the CT band and a small increase of heptalene bands II and III. Nevertheless, the photostationary state is established within 1 min with isosbestic points at 384 and 243 nm (*Fig. 19*).

The photodynamic process **23b** ⇌ **23a** changes completely in cyclohexane solution (*Fig. 20*). On irradiation with white light, the photostationary state is rapidly reached,

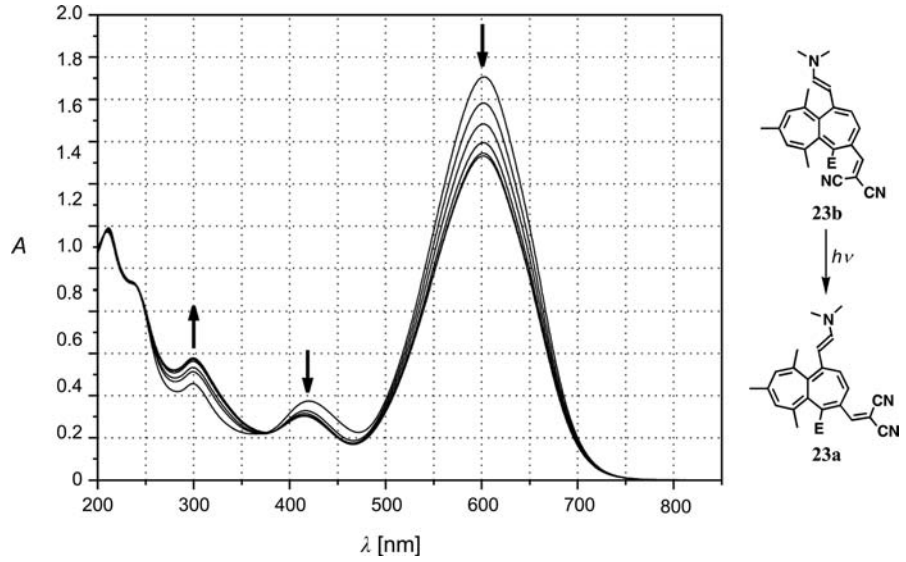

Fig. 19. *UV/VIS Spectra of the photoisomerization* **23b** → **23a** *in MeCN* ($\Delta t = 10$ s). E = COOMe.

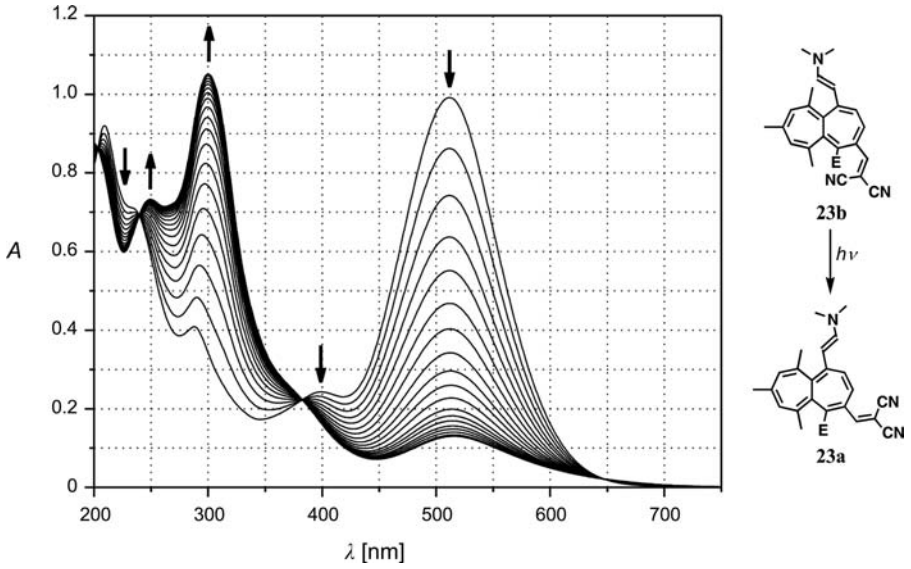

Fig. 20. *UV/VIS Spectra of the photoisomerization* **23b** → **23a** *in cyclohexane* ($\Delta t = 10$ s). E = COOMe.

whereby the CT band – shifted in comparison with MeCN (λ_{max} 614 nm) hypsochromically by 102 nm to 512 nm – is reduced by at least 87%. Clearly defined isosbestic points are found at 383 and 239 nm and just recognizable at 203 nm. Moreover, the weakly recognizable heptalene band II of **23b** vanishes almost completely at the expense of the strongly developing heptalene band III of **23a**, which shows virtually no solvent effect

(*cf. Figs. 19* and *20*). In *Fig. 21*, the spectrum of the photochemical equilibrium mixture of **23a**/**23b** in cyclohexane and its thermal development within 1 h are displayed. The equilibrium is far on the side of **23a** and does not move very much at room temperature; in other words, less polar **23a** is favored in nonpolar cyclohexane. On the other hand, the highly polar, almost zwitterionic **23b** is stabilized in polar MeCN, in a way that the photochemical equilibrium is far on the side of **23b**, in contrast to its less polar aldehyde precursor **19b** in MeCN, which exists in photo-equilibrated form mostly as its DBS isomer **19a** (*Fig. 15*).

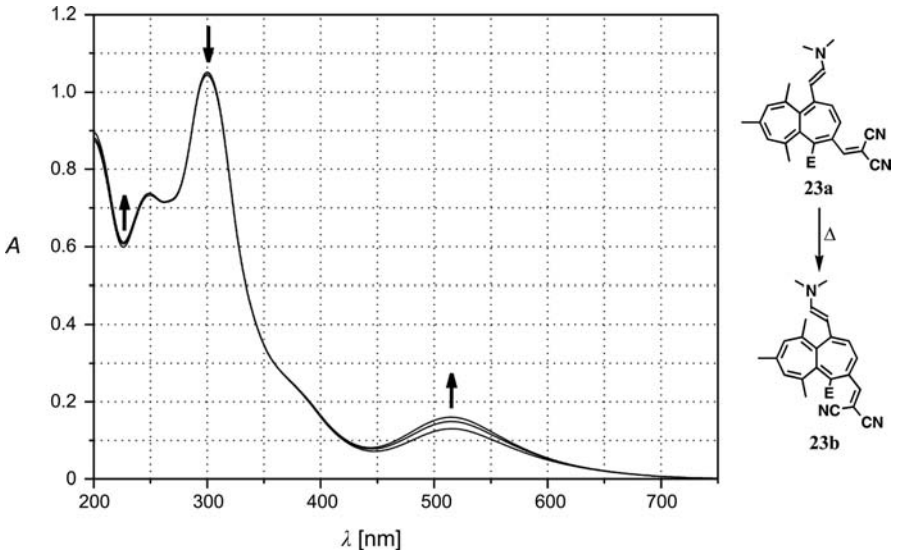

Fig. 21. *UV/VIS Spectra of the thermoisomerization* **23a** → **23b** *in cyclohexane* (r.t., $\Delta t = 0.5$ h). E = COOMe.

The intense heptalene band III of **23a** in the photostationary state with **23b** in cyclohexane on irradiation with white light (*cf.* also *Fig. 20*) allowed, on selective irradiation at 300 nm (light of a fluorescence tube (32 Watt) with λ_{emiss} 300 nm), the adjustment of a new photostationary state with **23b** in excess and well-defined isosbestic points at 381 and 242 nm (*Fig. 22*).

Finally, we investigated the photochemical behavior of the Me–C(5) analog **24b** of **23b** in MeCN (*Fig. 23*) and were quite surprised to find that it resembles those of **23b** in cyclohexane (*cf. Fig. 20*). The photostationary state is reached within 1 min, whereby the CT band of **24b** is reduced by 86% of its original value. Isosbestic points at 412 and 249 nm and a weakly recognizable at 205 nm document unambiguously the clean reversible transformation **24b** ⇌ **24a**. Heptalene band II of **24a** appears, as in the case of **23a**, as a well-defined shoulder at 371 nm, followed by the intense absorption of heptalene band III at 297 nm. When stored in the dark at room temperature, the photo-equilibrated mixture **24a**/**24b** turns back to **24b** (*Fig. 24*). After 210 min, the CT band of **24b** has attained already 93% of its original value of pure **24b**. This result has to be seen in the light of the thermal behavior of the progenitor of **24a**, carboxaldehyde **20a**, which

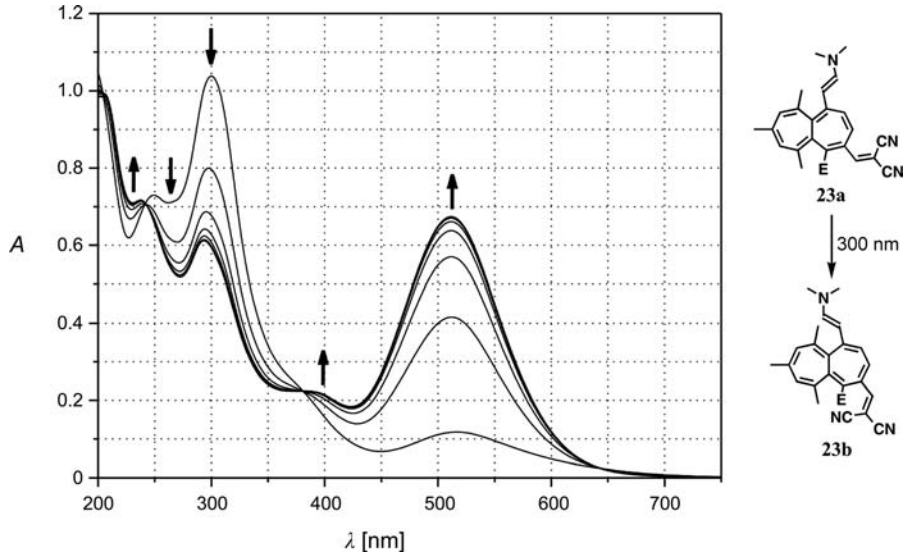

Fig. 22. *UV/VIS Spectra of the photoisomerization* **23a** → **23b** *in cyclohexane* ($\Delta t = 30$ s). E = COOMe.

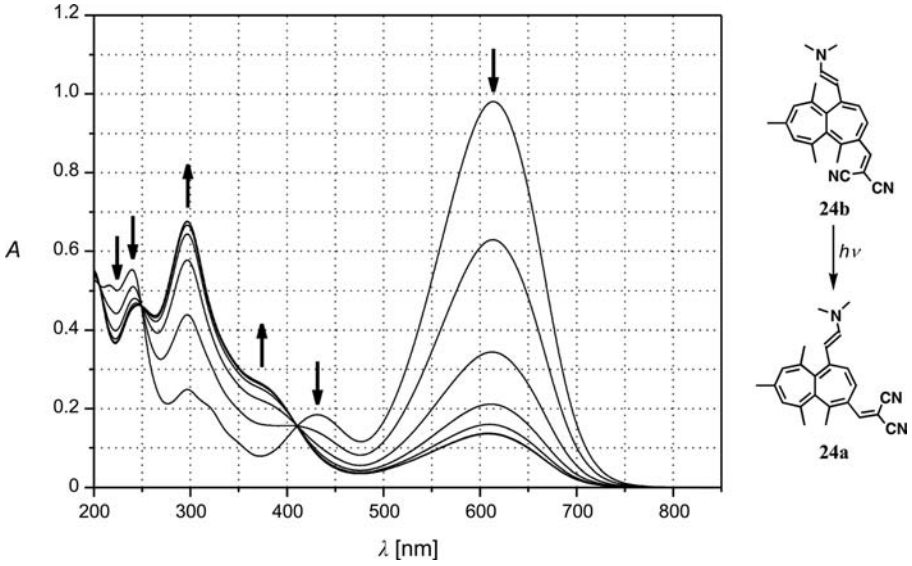

Fig. 23. *UV/VIS Spectra of the photoisomerization* **24b** → **24a** *in MeCN* ($\Delta t = 10$ s)

is formed on irradiation of **20b** in MeCN (*Fig. 17*). It undergoes only sluggishly the DBS process to **20b** (*Fig. 18*), indicating that the re-establishment of the almost ionic structure of **24b** is a strong driving force for the thermal π-bond shift **24a** → **24b** in polar MeCN.

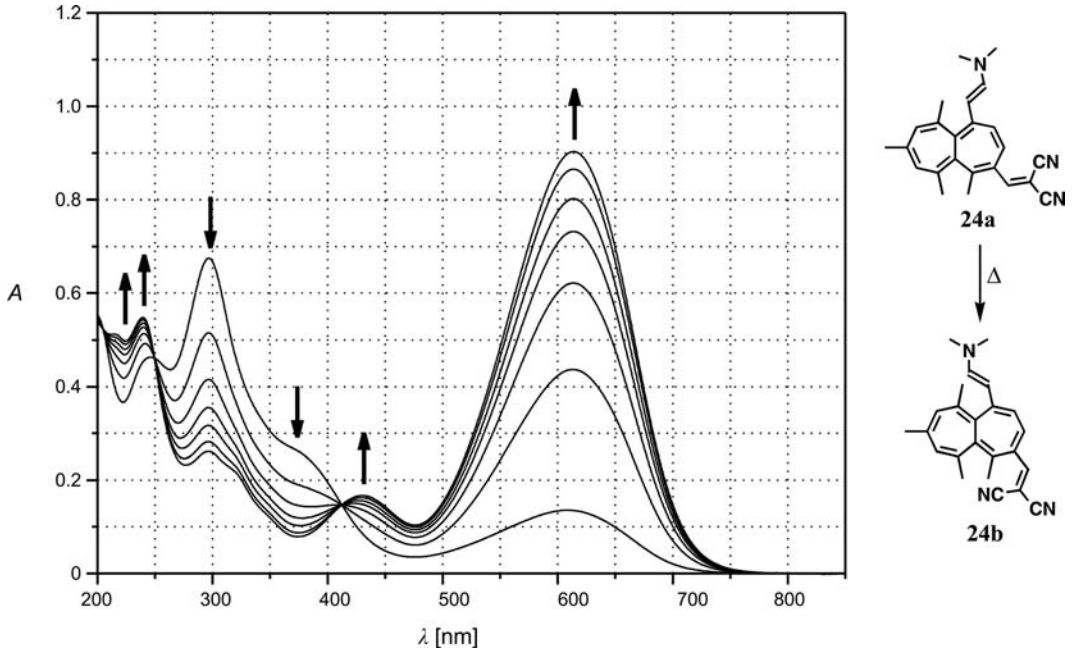

Fig. 24. *UV/VIS Spectra of the thermoisomerization* **24a** → **24b** *in MeCN* (r.t., $t = 0, 15, 30, 45, 60, 90, 150,$ and 210 min)

2.5.3. *1,2-Donor–Acceptor-Substituted Heptalenes.* The fundamental difference of carboxaldehyde **18a** and its malononitrile derivative **26a** with respect to the so far investigated heptalene-based merocyanines is that the two functional groups determining their merocyanine character are at neighboring C-atoms, so that they principally can interact also through space[12]). In addition, they absorb light at shorter wavelengths, and the strength of their CT bands are not as dominating as in the case of the 1,4-counterparts (*cf. Figs. 10* and *14*). The excitation energy in MeCN of the 1,4-merocyanine **20b** and its isomeric 1,2-analog **18a** differs by 2.5 kcal mol^{-1}, and it increases to 6.0 kcal mol^{-1} for their malononitrile derivatives **24b** and **26a**. The study of the photochemical behavior of the new 1,2-linked merocycyanines **18a** and **26a** under our standard conditions was therefore of great interest for us.

The course of the photochemical changes of **18a** in MeCN is displayed in *Fig. 25*. The photostationary state of **18a** ⇌ **18b** is reached after 8 min and leads to a reduction of heptalene band I by 39% in contrast to the behavior of its 1,4-analog **20b**, where the photo-equilibrated state is established after 2 min accompanied by a decrease of the CT band by 93% (*cf. Fig. 17*). The photochemically induced DBS process is thermally reversible as is indicated by the slow recovery of the CT band of the photo-equilibrated solution of **18a**/**18b** on storage in the dark. After 6 d, the CT band has increased again to 83% of its original value (*Fig. 26*).

---

[12]) Compounds with an integrated *cis*-hexa-1,3,5-triene structure show a rich photochemistry (see our former work [22] and refs. cit. therein).

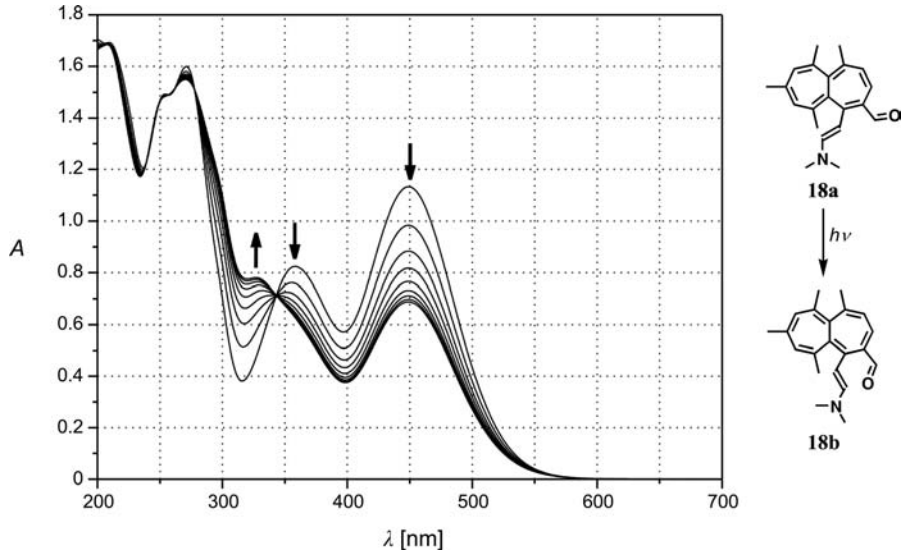

Fig. 25. *UV/VIS Spectra of the photoisomerization* **18a** → **18b** *in MeCN* ($\Delta t = 60$ s)

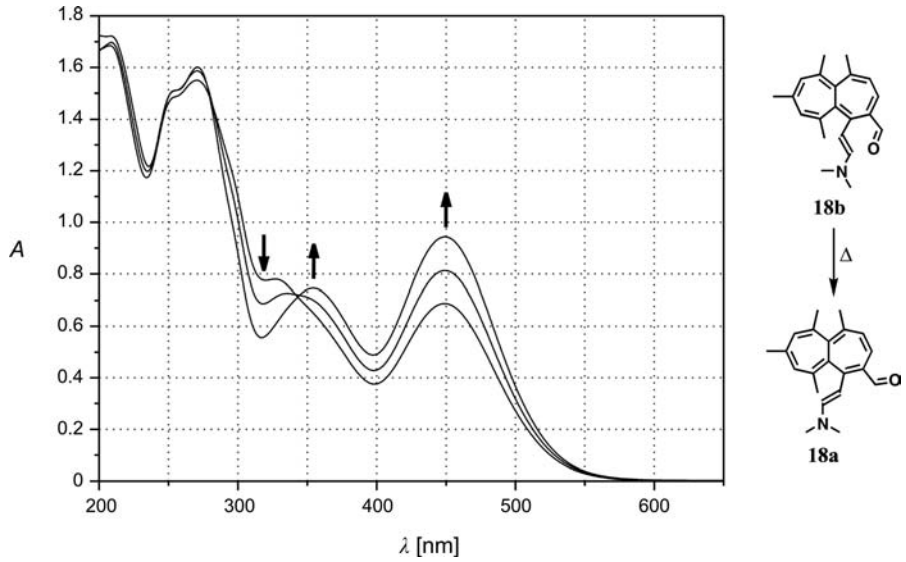

Fig. 26. *UV/VIS Spectra of the thermoisomerization* **18b** → **18a** *in MeCN* (r.t., $t = 0$, 2, and 6 d)

The DBS process is unambiguous in the excited state as well as in the ground-state as indicated by the same isosbestic points at 343 and 278 nm. Moreover, the photo-equilibration **18a** ⇌ **18b** can also be observed in cyclohexane with clearly defined isosbestic points at 334, 269, and 254 nm (*Fig. 27*). The photostationary state is reached after 12 min with a reduction of the CT band by 71%. The spectrum of the equilibrated state shows in the dark at room temperature no changes after 1 h.

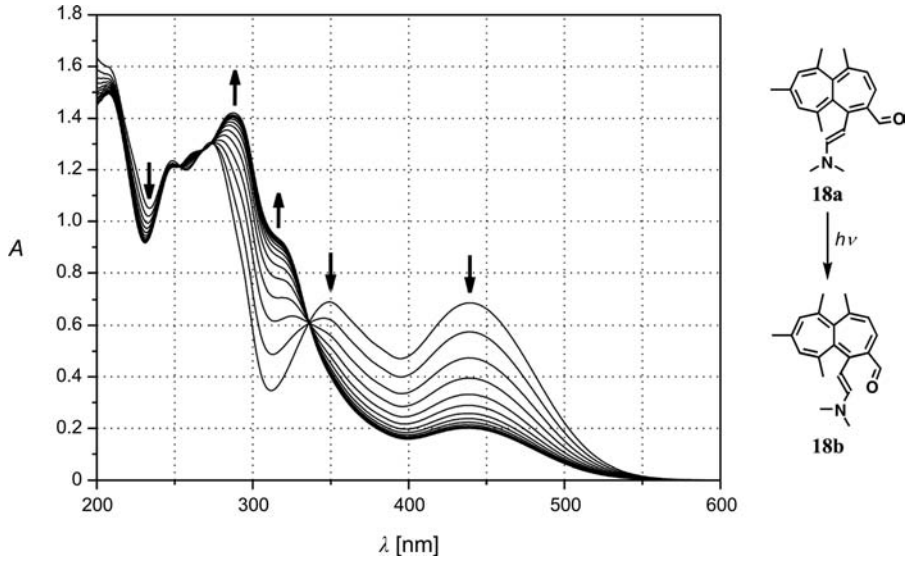

Fig. 27. *UV/VIS Spectra of the photoisomerization* **18a** → **18b** *in cyclohexane* ($\Delta t = 60$ s)

The irradiation of the malononitrile derivative **26a** of carboxaldehyde **18a** in MeCN was disappointing despite the fact that heptalene band I and II at 544 and 396 nm, respectively, decrease steadily within 3 min (*Fig. 28*). However, no clear isosbestic points can be made out. If the point of intersection after 0 and 15 s at 369 nm with

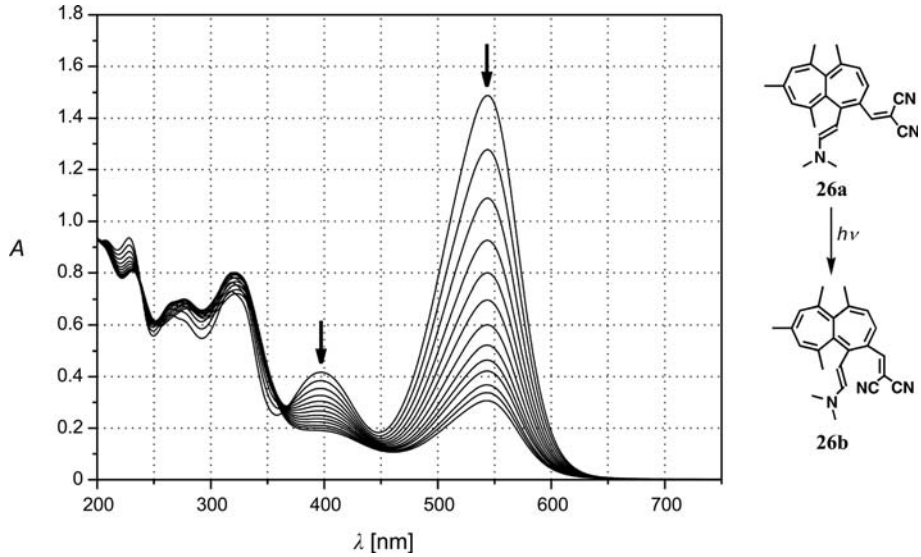

Fig. 28. *UV/VIS Spectra of the photoisomerization* **26a** → **26b** *in MeCN* ($\Delta t = 15$ s)

$A_{IP} = 0.29$ is taken as reference, all further spectral lines should pass this point with the same intensity. However, the measured extinction at this point decreases continuously in the course of the irradiation. Moreover, the spectra do not indicate the approach towards a photo-equilibrium. Beside or as a consequence of the photo-isomerization, a further reaction must therefore take place, which destroys the switching of the DBS system **26a** ⇌ **26b**.

The photo-isomerization of **26a** in cyclohexane runs cleaner with a clearer defined isosbestic point at 371 nm (*Fig. 29*). The photostationary state is reached after 3 min, whereby heptalene band I is reduced by only 29%, which indicates that the photo-equilibrium **26a** ⇌ **26b** is under the applied conditions still far on the side of **26a**.

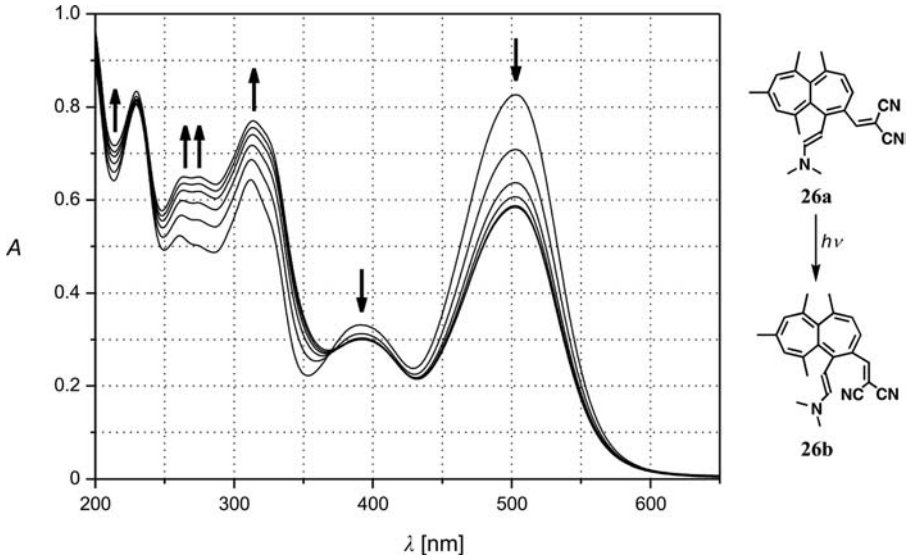

Fig. 29. *UV/VIS Spectra of the photoisomerization* **26a** → **26b** *in cyclohexane* ($\Delta t = 30$ s)

The discussed results show that heptalene based merocyanines with the (1*E*)-2-(dimethylamino)ethenyl moiety as donor part at C(1) and the carboxaldehyde or 2,2-dicyanoethenyl group as acceptor part at C(4) or C(2) of the heptalene skeleton are photochemically fully switchable by irradiation into the strong CT absorption (heptalene band I) of their through-conjugated forms. The thus established photostationary states can be thermally reverted to their starting position or shifted towards this point by selective irradiation into heptalene band III. Heptalenes with the donor and acceptor group in 1,4-position do the job much better than those with the groups at neighboring 1,2-position.

We thank our NMR laboratory for specific NMR measurements, our MS laboratory for mass spectra, and our laboratory for microanalysis. Financial support of this work by the *Swiss National Science Foundation* is gratefully acknowledged.

Experimental Part

General. See [7].

1. *Synthesis of Heptalenecarboxaldehydes.* 1.1. *1,5,6,8,10-Pentamethylheptalene-4-carboxaldehyde* (**4b**), *1,5,6,8,10-Pentamethylheptalene-2-carboxaldehyde* (**4a**), *and 2,5,6,8,10-Pentamethylheptalene-1-carboxaldehyde* (**8**) (*cf.* [8]). A soln. of 1,6,8,10-tetramethylheptalene-4,5-dimethanol (**7b**; 2.70 g, 10.0 mmol) [23][24] and $TsOH \cdot H_2O$ (0.19 g, 1.00 mmol) in dioxane (150 ml) was heated under reflux for 15 h (yellow → dark orange). Dioxane was evaporated, and the residual brown oil was separated by CC (silica gel (SiO_2), hexane/Et_2O 10:1). The deep yellow to orange fraction and the directly following red fraction were isolated. The yellow-orange fraction delivered, after removal of the solvent and drying under h.v., **4b**/**4a** (1.877 g, 74%), ratio 57:43 (by ^{1}H-NMR), as a yellow solid. This mixture was employed in all further experiments. The red fraction gave a red oil, which contained mainly **8** beside small amounts of **4a** and **4b**.

Data of **4b**: R_f (hexane/^{t}BuOMe 5:1) 0.56. ^{1}H-NMR (300 MHz, $CDCl_3$; in the presence of 43% of **4a**): 9.52 (*s*, CHO; NOE with Me–C(5) and H–C(3)); 7.05 (*d*, ^3J(3,2) = 5.8, H–C(3)); 6.34 (*dm*, ^3J(2,3) = 5.8, H–C(2)); 6.04 (*s*, H–C(9)); 5.98 (*s*, H–C(7)); 2.06 (*d*, ^4J(Me–C(1),2) = 1.0, Me–C(1)); 2.01 (*d*, ^4J(Me–C(6),7) = 1.3, Me–C(6)); 1.98 (*s*, Me–C(8)); 1.97 (*s*, Me–C(5)); 1.70 (*s*, Me–C(10)).

Data of **4a**: R_f (hexane/^{t}BuOMe 5:1) 0.51. ^{1}H-NMR (300 MHz, $CDCl_3$; in the presence of 57% of **4b**): 10.17 (*s*, CHO; NOE with Me–C(1) and H–C(3)); 6.82 (*d*, ^3J(3,4) = 11.8, H–C(3)); 6.39 (*d*, ^3J(4,3) = 11.8, H–C(4)); 6.13 (*s*, H–C(9)); 6.01 (*s*, H–C(7)); 2.36 (*s*, Me–C(1)); 2.00 (*d*, ^4J(Me–C(8),9) = 1.3, Me–C(8)); 1.98 (*d*, ^4J(Me–C(6),7) = 1.3, Me–C(6)); 1.74 (*s*, Me–C(5)); 1.73 (*s*, Me–C(10)).

Data of **8**: R_f (hexane/^{t}BuOMe 5:1) 0.46. ^{1}H-NMR (300 MHz, $CDCl_3$): 9.82 (*s*, CHO; NOE with Me–C(2) and Me–C(10)); 6.53 (*d*, ^3J(4,3) = 11.7, H–C(4)); 6.39 (*d*, ^3J(3,4) = 11.7, H–C(3)); 6.15 (*s*, H–C(9)); 6.07 (*s*, H–C(7)); 2.40 (*s*, Me–C(2)); 2.00 (*d*, ^4J(Me–C(8),9) = 1.2, Me–C(8)); 1.94 (*d*, ^4J(Me–C(6),7) = 1.3, Me–C(6)); 1.78 (*s*, Me–C(5)); 1.56 (*s*, Me–C(10)).

1.2. *4-(Hydroxymethyl)-5,6,8,10-tetramethylheptalene-1-carboxaldehyde* (**13b**). 1.2.1. *Dimethyl 1-[(Acetyloxy)methyl]-6,8,10-trimethylheptalene-4,5-dicarboxylate* (**10b**). Under dry N_2, dimethyl 1-(chloromethyl)-6,8,10-trimethylheptalene-4,5-dicarboxylate (**9b**; 0.341 g, 0.945 mmol) [1] was dissolved in DMSO (15 ml; dried over CaH_2). Dry AcOK (0.464 g, 4.73 mmol) was added, and the mixture was stirred for 4 d at r.t., whereby most of the acetate was dissolved (orange → olive-green). H_2O was added and the mixture extracted with ^{t}BuOMe. The combined extract was washed several times with H_2O and finally with aq. sat. NaCl soln. dried (Na_2SO_4), and concentrated, and the orange oil purified by CC (SiO_2, hexane/^{t}BuOMe 10:1 → 1:10). The thus obtained yellow oil formed a stiff foam on drying under h.v.: **10b** (0.223 g, 61%). Brittle yellow solid. Glass point *ca.* 36°. R_f (hexane/^{t}BuOMe 2:1) 0.18; R_f (hexane/AcOEt 1:1) 0.68. UV/VIS (MeCN): max. 322 (sh, 3.47), 263 (4.18), 209 (4.40); min. 245 (4.14). IR (KBr): 2948*m*, 2919*m*, 2856*w*, 1750 (sh), 1722v*s* and 1703v*s* (C=O), 1646*m*, 1624*w*, 1604*w*, 1574*m*, 1530*w*, 1435*s*, 1396*w*, 1375*m*, 1299*s*, 1268v*s*, 1246v*s*, 1217v*s*, 1194*s*, 1155*m*, 1089*s*, 1051*s*, 1025*m*, 1002*m*, 970*m*, 948*w*, 921*w*, 885*w*, 874*w*, 856*m*, 841*m*, 823*w*, 802*w*, 785*m*, 773*m*, 700*w*, 649*w*, 621*w*, 602*w*, 549*w*. ^{1}H-NMR (300 MHz, $CDCl_3$): 7.58 (*dm*, ^3J(3,2) = 5.8, H–C(3)); 6.46 (*dm*, ^3J(2,3) = 5.8, H–C(2)); 6.14 (*s*, H–C(7 or 9)); 6.02 (*s*, H–C(9 or 7)); 4.73 and 4.54 (*dm*, ^2J = 14.6, OCH_2–C(1)); 3.72 (*s*, COOMe); 3.69 (*s*, COOMe); 2.08 (*s*, MeOOC–C(1)); 2.05 (*d*, ^4J = 1.2, Me); 2.00 (*d*, ^4J = 1.2, Me); 1.76 (*s*, Me). ^{13}C-NMR (75 MHz, $CDCl_3$): 170.25 (*s*, C=O); 167.58 (*s*, C=O); 167.33 (*s*, C=O); 146.95 (*s*); 140.38 (2*s*); 138.38 (*d*); 133.06 (*s*); 132.40 (*s*); 130.83 (*s*); 129.97 (*d*); 129.40 (*d*); 126.24 (*d*); 122.68 (*s*); 120.79 (*s*); 65.04 (*t*, OCH_2–C(1)); 52.21 (*q*, COO*Me*); 51.98 (*q*, COO*Me*); 25.17 (*q*); 22.38 (*q*); 20.84 (*q*); 18.52 (*q*). CI-MS (NH_3): 402 (58, $[M + NH_4]^+$), 385 (5, $[M + H]^+$), 353 (25, $[M - MeO]^+$), 344 (12), 325 (100, $[M - COOMe]^+$), 295 (13), 228 (11). Anal. calc. for $C_{22}H_{24}O_6$ (384.43): C 68.74, H 6.29; found: C 68.59, H 6.38.

1.2.2. *6,8,10-Trimethylheptalene-1,4,5-trimethanol* (**11b**). Under Ar, **10b** (0.470 g, 1.22 mmol) was dissolved in THF (20 ml) and the soln. cooled to 0°. A 1M DIBAH soln. in cyclohexane (10 ml) was slowly added and stirring continued for 1 h at 0°. Thereafter, 1M aq. HCl (11 ml) was added under cooling and vigorous stirring. After 5 min, AcOEt (50 ml) was added and stirring continued (10 min) at r.t. The yellow org. phase was washed and dried in the usual manner. After evaporation of AcOEt, the residual yellow oil solidified by scratching in the presence of a small amount of CH_2Cl_2. The yellow solid was filtered off and dried under h.v.: **11b** (0.194 g, 56%). M.p. 154–156° (MeOH). R_f (AcOEt/hexane 10:1)

0.39. UV/VIS (MeCN): max. 302 (sh, 3.47), 254 (4.31), 242 (sh, 4.23), 203 (4.34); min. 228 (4.03). IR (KBr): 3301v*s*, 2967*s*, 2935*s*, 2908*s*, 2855*s*, 2725*w*, 1649*m*, 1625*w*, 1606*w*, 1563*w*, 1438*s*, 1372*m*, 1344*m*, 1244*m*, 1220*m*, 1174*w*, 1139*m*, 1115*m*, 1094*w*, 1065*s*, 1001v*s*, 906*w*, 846*s*, 801*w*, 763*m*, 736*m*, 677*m*, 620*m*, 545*w*, 478*w*. ^{1}H-NMR (300 MHz, (D_6)acetone): 6.58 (*d*, ^3J = 6.0, H–C(3)); 6.41 (*dm*, ^3J = 6.0, H–C(2)); 6.02 (*s*, H–C(7 or 9)); 5.97 (*s*, H–C(9 or 7)); 4.34 – 3.90 (*m*, 3 CH_2OH); 2.07 (*d*, ^4J = 1.3, Me); 1.92 (*d*, ^4J = 1.2, Me); 1.64 (*s*, Me–C(10)). ^{13}C-NMR (75 MHz, (D_6)acetone): 143.04 (*s*); 141.26 (*s*); 138.80 (*s*); 137.62 (*s*); 132.26 (*s*); 131.21 (*d*); 131.10 (*d*); 129.87 (*d*); 129.86 (*s*); 129.22 (*s*); 127.74 (*s*); 124.42 (*d*); 66.77, 64.00, 59.31 (3*t*, 3 CH_2OH); 24.81 (*q*); 24.17 (*q*); 18.19 (*q*). CI-MS (NH_3): 304 (6, [*M* + NH_4]$^+$), 269 (100, [*M* – OH]$^+$), 253 (11), 251 (12, [*M* – (H_2O + OH)]$^+$), 175 (18), 102 (13).

1.2.3. *Acid-Catalyzed Disproportionation of* **11b**: *4-(Hydroxymethyl)-5,6,8,10-tetramethylheptalene-1-carboxaldehyde* (**13b**). A soln. of **11b** (14.4 mg, 0.050 mmol) and a trace of TsOH · H_2O (amount of a micro-spatula tip) in diglyme (2.5 ml) was heated under reflux for 10 min. After cooling, the mixture was diluted with AcOEt. The soln. was washed and finally dried in the usual manner. A small amount of SiO_2 was added before the solvents were evaporated. The thus adsorbed crude product was purified by CC (SiO_2, hexane/AcOEt 10 : 1 → 1 : 1). The orange fraction was collected and the solvent mixture evaporated. The residual oil was treated with a small amount of Et_2O. Scratching with a glass rod gave crystals of **13b** (5.2 mg, 39%). Orange prisms. M.p. 192 – 194° (Et_2O). R_f (hexane/AcOEt 1 : 1) 0.62. UV/VIS (MeCN): max. 415 (2.96), 271 (4.22), 240 (4.20), 211 (4.29); min. 364 (2.78), 259 (4.20), 231 (4.19), 203 (4.28). IR (KBr): 3449*s* (O–H), 3285 (sh, O–H), 2967*m*, 2940*m*, 2912*m*, 2846*m*, 2830*m* and 2729*w* (CHO), 1653v*s* (C=O), 1600*s*, 1586*s*, 1558*m*, 1514*s*, 1438*s*, 1414*m*, 1369*s*, 1288*w*, 1242*w*, 1207*s*, 1195*m*, 1139*m*, 1123*m*, 1103*s*, 1048*m*, 1025*m*, 1008*s*, 979*w*, 963*w*, 923*w*, 863*m*, 850*s*, 788*w*, 764*m*, 705*w*, 683*w*, 650*w*, 640*w*, 586*m*, 552*w*, 512*w*, 488*w*, 470*w*. ^{1}H-NMR (300 MHz, $CDCl_3$): 9.53 (*s*, CHO); 7.13 (*d*, ^3J(2,3) = 6.2, H–C(2)); 6.77 (*dm*, ^3J(3,2) = 6.2, H–C(3)); 6.10 (*s*, H–C(9)); 6.03 (*s*, H–C(7)); 4.51 (*dd*, ^2J = 14.4, ^3J(CH_2–C(4),OH) = 5.8, 1 H, CH_2–C(4)); 4.35 (*dd*, ^2J = 14.4, ^3J(CH_2–C(4),OH) = 6.0, 1 H, CH_2–C(4)); 1.99 (*d*, ^4J(Me–C(8),9) = 1.2, Me–C(8)); 1.92 (*d*, ^4J(Me–C(6),7) = 1.3, Me–C(6)); 1.79 (*s*, Me–C(5)); 1.64 (*t*, ^3J(OH,CH_2–C(4)) = 6.0, CH_2O*H*); 1.54 (*s*, Me–C(10)). ^{13}C-NMR (75 MHz, $CDCl_3$): 190.10 (*d*, CHO); 151.20 (*s*); 145.44 (*d*); 141.12 (*s*); 139.21 (*s*); 136.57 (*s*); 131.48 (*s*); 131.12 (*s*); 130.04 (*d*); 129.93 (*d*); 127.59 (*s*); 124.71 (*d*); 120.78 (*s*); 65.97 (*t*, CH_2OH); 24.84 (*q*); 22.58 (*q*); 17.86 (*q*); 14.26 (*q*). CI-MS: 269 (100, [*M* + H]$^+$), 253 (9, [*M* – Me]$^+$), 251 (9, [*M* – OH]$^+$). Anal. calc. for $C_{18}H_{20}O_2$ (268.36): C 80.56, H 7.51; found: C 80.40, H 7.56.

The final structure of **13b** was verified by an X-ray crystal-structure analysis (*cf. Fig. 2* and *Table 8*).

1.3. *Methyl 4-Formyl-1,6,8,10-tetramethylheptalene-5-carboxylate* (**15b**). Under Ar, 1,1-dimethoxy-6,7,9,11-tetramethylheptaleno[4,5-*c*]furan-3(1*H*)-one (**14b**; 1.08 g, 3.30 mmol) [22] was dissolved in toluene (100 ml) and cooled to – 78°. At – 78°, a 1M DIBAH soln. in toluene (5.0 ml) was added dropwise. Shortly after, MeOH (5 ml), cooled to – 78°, was added to the orange soln. (→ yellow). After 5 min, the mixture was poured into H_2O under vigorous stirring. ^{t}BuOMe was added, followed by dropwise addition of conc. HCl soln. until two phases were clearly recognizable. The org. layer was successively washed with 1M aq. HCl, sat. aq. $NaHCO_3$ soln., H_2O, and sat. aq. NaCl soln. After drying (Na_2SO_4), the solvents were evaporated, and the residual orange oil was purified by CC (SiO_2, hexane/^{t}BuOMe 5 : 1 → 1 : 1): **15b** (0.698 g, 71%) which was washed with a small portion of pentane and then dried under h.v. Yellow solid. M.p. 141 – 144° (hexane/^{t}BuOMe). R_f (hexane/^{t}BuOMe 2 : 1) 0.28. UV/VIS (MeCN): max. 381 (sh, 2.97), 287 (sh, 4.17), 268 (4.20), 213 (4.38); min. 246 (4.12). IR (KBr): 3006*w*, 2978*w*, 2944*m*, 2909*m*, 247*w*, 2781*w* and 2738*w* (CHO), 1733v*s* (C=O, aldehyde), 1684v*s* (C=O, ester), 1645*m*, 1617*m*, 1594*w*, 1564*m*, 1530*m*, 1438*s*, 1422*m*, 1379*m*, 1346*w*, 1248v*s*, 1215*m*, 1202*s*, 1189*m*, 1174*m*, 1124*m*, 1110*m*, 1061*s*, 1044*m*, 1000*w*, 969*w*, 955*w*, 901*m*, 870*w*, 848*s*, 827*w*, 789*m*, 739*w*, 723*w*, 705*w*, 679*w*, 638*w*, 595*w*, 554*w*, 505*w*, 479*w*. ^{1}H-NMR (300 MHz, $CDCl_3$): 9.39 (*s*, CHO; NOE with H–C(3)); 7.16 (*d*, ^3J(3,2) = 5.7, H–C(3)); 6.42 (*dm*, ^3J(2,3) = 5.7, H–C(2)); 6.12 (*s*, H–C(7 or 9)); 6.02 (*s*, H–C(9 or 7)); 3.71 (*s*, COOMe); 2.05 (*d*, ^4J = 1.2, Me); 2.03 (*d*, ^4J = 1.3, Me); 1.97 (*d*, ^4J = 1.3, Me); 1.75 (*s*, Me–C(8)). ^{13}C-NMR (75 MHz, $CDCl_3$): 192.62 (*d*, CHO); 167.75 (*s*, *C*OOMe); 147.52 (*d*); 146.15 (*s*); 145.24 (*s*); 139.95 (*s*); 139.85 (*s*); 131.17 (*s*); 130.80 (*s*); 130.32 (*d*); 129.73 (*d*); 126.08 (*d*); 125.65 (*s*); 121.42 (*s*); 52.09 (*q*, COO*Me*); 25.05 (*q*); 23.89 (*q*); 22.01 (*q*); 18.46 (*q*). EI-MS: 296 (100, $M^{+\cdot}$), 281 (35, [*M* – Me]$^+$), 265 (10), 249 (19), 237 (21, [*M* – $C_2H_3O_2$]$^+$), 221 (18), 209 (14), 207 (16), 193 (38), 184 (63), 179 (37), 178

Table 8. *Crystallographic Data for Compounds* **13b**, **18a**, **23b**, **24b**, **26a**, **27**, *and* **28b**

	13b	**18a**	**23b**	**24b**	**26a**	**27**	**28b**
Crystallized from	Et_2O	Et_2O/hexane	hexane/AcOEt	CH_2Cl_2	hexane/AcOEt	THF/hexane	Et_2O/hexane
Empirical formula	$C_{18}H_{20}O_2$	$C_{21}H_{25}NO$	$C_{25}H_{25}N_3O_2$	$C_{24}H_{25}N_3$	$C_{24}H_{25}N_3$	$C_{24}H_{25}N_3$	$C_{18}H_{18}O_2$
M_r	268.35	307.43	399.49	355.48	355.48	355.48	266.34
Crystal color, habit	orange, prism	wine-red, prism	green, needle	metallic-bronze, prism	metallic-green, plate	metallic-green, prism	orange, prism
Crystal dimensions [mm]	$0.20 \times 0.38 \times 0.42$	$0.20 \times 0.20 \times 0.30$	$0.10 \times 0.17 \times 0.50$	$0.15 \times 0.15 \times 0.25$	$0.08 \times 0.25 \times 0.25$	$0.20 \times 0.25 \times 0.25$	$0.20 \times 0.33 \times 0.45$
Temperature [K]	173(1)	160(1)	160(1)	160(1)	160(1)	160(1)	153(1)
Crystal system	monoclinic	triclinic	triclinic	monoclinic	monoclinic	monoclinic	monoclinic
Space group	$P2_1/c$	$P\bar{1}$	$P\bar{1}$	$P2_1/n$	$P2_1/c$	$P2_1/n$	$P2_1/c$
Z	4	2	2	4	4	4	4
Reflections for cell determination	25	5131	6122	6026	6506	6340	21
2θ Range for cell determination [°]	37 – 40	4 – 60	4 – 60	4 – 60	2 – 60	4 – 60	31 – 39
Unit cell parameters:							
a [Å]	8.073(2)	8.2578(1)	9.8867(1)	6.8632(1)	11.4307(2)	11.6647(2)	8.061(2)
b [Å]	16.003(3)	8.7514(1)	10.5990(2)	14.0384(2)	12.4838(2)	11.8696(2)	16.075(2)
c [Å]	11.754(2)	13.8367(1)	11.7983(2)	20.8002(3)	15.8207(3)	15.8356(3)	11.583(2)
α [°]	90	73.2917(5)	68.2965(6)	90	90	90	90
β [°]	105.46(2)	85.6599(5)	69.7392(6)	97.5261(7)	109.1133(7)	108.4151(9)	108.24(2)
γ [°]	90	66.9654(4)	86.1086(8)	90	90	90	90
V [Å^3]	1463.7(5)	880.60(2)	1075.04(3)	1986.80(5)	2133.14(7)	2080.25(6)	1425.6(5)
$F(000)$	576	332	424	760	760	760	568
D_x [g cm^{-3}]	1.218	1.159	1.234	1.188	1.107	1.135	1.241
$\mu(\mathrm{Mo}K_\alpha)$ [mm^{-1}]	0.0776	0.0702	0.0794	0.0705	0.0657	0.0673	0.0794
Scan type	$\omega/2\theta$	ϕ and ω	ϕ and ω	ϕ and ω	ϕ and ω	ϕ and ω	$\omega/2\theta$
$2\theta_{(max)}$ [°]	55	60	60	60	60	60	55
Total reflections measured	3741	32355	27461	47689	54549	53356	3626
Symmetry-independent reflections	3374	5147	6230	5803	6243	6073	3269
R_{int}	0.042	0.041	0.045	0.062	0.069	0.041	0.028

Table 8 (cont.)

	13b	**18a**	**23b**	**24b**	**26a**	**27**	**28b**
Reflections with $I > 2\sigma(I)$	1942	3968	4619	3839	3640	4719	2117
Parameters refined	182	217	272	245	245	245	254
$R(F)$ ($I > 2\sigma(I)$ reflections)	0.0588	0.0542	0.0530	0.0519	0.0627	0.0641	0.0482
$wR(F)$ ($I > 2\sigma(I)$ reflections)	0.0510	0.0592	0.0597	0.0525	0.0690	0.0690	0.0421
Weights: p in $w = [\sigma^2(F_o) + (pF_o)^2]^{-1}$	0.005	0.005	0.005	0.013	0.005	0.005	0.005
Goodness of fit	2.300	3.658	2.699	1.825	3.324	4.348	1.593
Secondary extinction coefficient	–	–	$3.1(9) \cdot 10^{-6}$	$1.5(4) \cdot 10^{-6}$	$1.3(3) \cdot 10^{-6}$	$3.1(6) \cdot 10^{-6}$	$7(2) \cdot 10^{-7}$

(57), 165 (39), 152 (29), 128 (11), 115 (15), 89 (14), 59 (12, $C_2H_3O_2^+$), 43 (16). Anal. calc. for $C_{19}H_{20}O_3$ (296.37): C 77.00, H 6.80; found: C 77.28, H 7.03.

1.4. *5,6,8,10-Tetramethylheptalene-1,4-dicarboxaldehyde* (**28b**) *and 1,6,8,10-Tetramethylheptalene-2,5-dicarboxaldehyde* (**28a**). 1.4.1. *Method A:* Under Ar, **13b** (22.3 mg, 0,083 mmol) was dissolved in dry CH_2Cl_2 and mixed with powdered molecular sieve (100 mg). To this stirred mixture, 4-methylmorpholine 4-oxide monohydrate (NMO; 26.8 mg, 0.198 mmol) and tetrapropylammonium perruthenate (TPAP; 4.5 mmg, 0.013 mmol) were added in small portions within 15 min at r.t. (→ dark mixture). The mixture was filtered over SiO_2, the filter cake washed with CH_2Cl_2 until it became colorless, the orange filtrate concentrated, and the residue subjected to CC (SiO_2, hexane/^{t}BuOMe 2:1): **28b**/**28a** (15.5 mg, 70%), ratio 72:28 (by ^{1}H-NMR). Micro-crystalline orange solid.

Data of **28b**: See *1.4.2* (*Method B*).

Data of **28a**: ^{1}H-NMR (300 MHz, $CDCl_3$; in a mixture with 72% **28b**): 10.18 (*s*, CHO); 9.87 (*s*, CHO); 7.01 (*d*, ^3J = 12.0, H–C(2 or 3)); 6.87 (*d*, ^3J = 12.0, H–C(3 or 2)); 6.26 (*s*, H–C(7 or 9)); 6.22 (*s*, H–C(9 or 7)); 2.39 (*s*, Me); 2.24 (*d*, ^4J = 1.3, Me); 2.06 (*d*, ^4J = 1.2, Me); 1.82 (*s*, Me–C(10)).

1.4.2. *Method B:* $NaIO_4$ (0.193 g, 0.90 mmol) and (aminoethenyl)heptalenecarboxaldehyde **20b** (0.092 g, 0.30 mmol) were dissolved in 50% aq. THF (10ml) and stirred at r.t. for 90 min (deep red → orange soln. and colorless solid). The suspension was filtered over a glass frit and the filter cake washed with AcOEt until it became colorless. The AcOEt phase of the two-phase filtrate was washed with sat. aq. $NaHCO_3$ soln., H_2O, and finally sat. aq. NaCl soln., dried (Na_2SO_4), and concentrated, the residue dissolved in ^{t}BuOMe, this soln. again concentrated, and the product precipitated with pentane and dried under h.v.: **28b** (0.070 g, 96%). Red prisms. M.p. 195–197° (CH_2Cl_2/^{t}BuOMe). R_f (hexane/AcOEt 1:1) 0.78. UV/VIS (MeCN): max. 456 (2.87), 278 (4.28), 211 (4.31); min. 397 (2.71), 249 (4.12). IR (KBr): 2972*m*, 2944*m*, 2910*m*, 2841*m*, 2767*w* and 2718*w* (CHO), 1690v*s* and 1674v*s* (C=O), 1622*w*, 1604*w*, 1587*w*, 1556*w*, 1525*w*, 1439*m*, 1375*m*, 1344*m*, 1286*w*, 1205*s*, 1187*m*, 1131*m*, 1119*m*, 1086*w*, 1045*m*, 1025*w*, 999*w*, 917*w*, 864*m*, 853*s*, 801*m*, 787*s*, 734*w*, 715*w*, 702*w*, 640*w*, 592*m*, 536*w*, 524*w*, 481*w*. ^{1}H-NMR (300 MHz, $CDCl_3$): 9.73 (*s*, CHO); 9.61 (*s*, CHO); 7.32 (*d*, ^3J = 6.0, H–C(2 or 3)); 7.28 (*d*, ^3J = 6.0, H–C(3 or 2)); 6.10 (*s*, H–C(7 or 9)); 6.04 (*s*, H–C(9 or 7)); 2.00 (*d*, ^4J = 1.1, Me); 1.98 (*s*, Me); 1.96 (*d*, ^4J = 1.3, Me); 1.54 (*s*, Me). ^{13}C-NMR (75 MHz, $CDCl_3$): 193.40 (*d*, CHO); 189.79 (*d*, CHO); 147.15 (*s*); 143.29 (*s*); 142.01 (*d*); 141.33 (*d*); 141.15 (*s*); 140.15 (*s*); 132.97 (*s*); 131.13 (*s*); 130.35 (*d*); 129.96 (*d*); 126.38 (*s*); 120.00 (*s*); 24.88 (*q*); 22.06 (*q*); 17.90 (*q*); 14.28 (*q*). EI-MS: 266 (74, $M^{+\cdot}$), 251 (100, $[M-Me]^+$), 237 (14, $[M-CHO]^+$), 207 (14), 197 (15), 194 (24), 179 (62), 165 (55), 152 (25), 128 (14), 115 (17), 91 (11), 77 (13), 51 (12). Anal. calc. for $C_{18}H_{18}O_2$ (266.34): C 81.17, H 6.81; found: C 81.47, H 6.80.

The final structure of **28b** was secured by an X-ray crystal-structure analysis (*Fig. 9* and *Table 8*).

2. *Aminoethenylation of the Heptalenecarboxaldehydes.* 2.1. *1-[(1*E*)-2-(Dimethylamino)ethenyl]-5,6,8,10-tetramethylheptalene-2-carboxaldehyde* (**18a**). To **4b**/**4a** (0.254 g, 1.0 mmol) in dry DMF was added dimethylformamide dimethyl acetal (DMFDMA; 0.5 ml, 3.8 mmol) and Et_3N (0.14 ml, 1.0 mmol). The orange soln. was heated under stirring at 80° for 24 h. The now red soln. was poured into H_2O and extracted with AcOEt (3×). The usual workup procedure led to a dark red compound, which was purified by CC (SiO_2, hexane/Et_2O 5:1 → 1:5). The red fraction delivered dark red crystals, which were dried under h.v.: **18a** (0.174 g, 57%). Red prisms. M.p. 165–167° (hexane/Et_2O). R_f (hexane/AcOEt 1:1) 0.47. UV/VIS (MeCN; *Fig. 14*): max. 449 (4.17), 358 (4.03), 271 (4.32), 254 (4.29), 209 (4.34); min. 397 (3.87), 316 (3.69), 257 (4.29), 236 (4.19). IR (KBr): 3064*w*, 3003*m*, 2972*m*, 2936*m*, 2910*m*, 2854*m*, 2738*w* and 2679*w* (CHO), 1639v*s* (C=O), 1599v*s*, 1558*s*, 1540*s*, 1496*s*, 1471*s*, 1439*s*, 1381v*s*, 1355*s*, 1329*m*, 1283*s*, 1260*s*, 1199*s*, 1184*s*, 1167*m*, 1138*m*, 1105v*s*, 1065*m*, 1025*w*, 987*w*, 959*m*, 930*w*, 864*w*, 842*m*, 800*w*, 786*s*, 769*m*, 752*m*, 727*w*, 690*w*, 649*w*, 624*w*, 602*w*, 575*w*, 557*w*, 504*w*, 468*w*. ^{1}H-NMR (300 MHz, $CDCl_3$): 9.89 (*s*, CHO); 6.80 (*d*, ^3J (3,4) = 11.5, H–C(3)); 6.66 (*d*, ^3J(2′,1′) = 12.7, H–C(2′)); 6.23 (*d*, ^3J(1′,2′) = 12.7, H–C(1′)); 6.15 (*s*, H–C(9)); 6.07 (*s*, H–C(7)); 6.05 (*d*, ^3J(4,3) = 11.5, H–C(4)); 2.90 (*s*, Me_2N); 2.01 (*d*, ^4J(Me–C(8),9) = 1.2, Me–C(8)); 1.87 (*d*, ^4J(Me–C(6),7) = 1.3, Me–C(6)); 1.74 (*s*, Me–C(5)); 1.65 (*s*, Me–C(10)). ^{13}C-NMR (75 MHz, $CDCl_3$): 188.46 (*d*, CHO); 149.76 (*d*); 148.18 (*s*); 137.89 (*s*); 134.36 (*s*); 132.96 (*s*); 130.14 (*d*); 129.29 (*d*); 129.07 (*s*); 128.49 (*d*); 128.40 (*d*); 127.60 (*s*); 127.31 (*s*); 123.95 (*s*); 93.52 (*d*); 41.11 (2*q*, Me_2N); 25.00 (*q*); 21.07 (*q*); 17.99 (*q*); 17.84 (*q*). CI-MS (NH_3): 308 (100, $[M+H]^+$). EI-MS: 307 (100, $M^{+\cdot}$), 292 (10, $[M-Me]^+$), 279 (12), 264 (25), 249 (26), 234 (11),

224 (13), 219 (15), 210 (21), 193 (16), 189 (18), 184 (42), 169 (19), 165 (21), 115 (15), 94 (11), 91 (11), 72 (16). Anal. calc. for $C_{21}H_{25}NO$ (307.44): C 82.04, H 8.20, N 4.56; found: C 81.94, H 8.37, N 4.49.

The structure of **18a** was finally established by an X-ray crystal-structure analysis (*Fig. 3*, *Table 8*).

2.2. *Methyl 1-[(1*E*)-2-(Dimethylamino)ethenyl]-4-formyl-6,8,10-trimethylheptalene-5-carboxylate* (**19b**). Under Ar, **15b** (0.446 g, 1.50 mmol) was treated with DMFDMA (1.0 ml, 7.50 mmol) in dry DMF (20 ml) at 110° for 4 h. The resulting deep red soln. was diluted with ^{t}BuOMe and washed in the usual manner. After drying, a small amount of SiO_2 and Et_3N was added before evaporation of ^{t}BuOMe. The thus adsorbed crude product was purified by CC (SiO_2, hexane/^{t}BuOMe 1:1 → 1:4 with a trace of Et_3N as additive). The obtained dark red solid was re-dissolved in a minimum amount of CH_2Cl_2 and precipitated by isothermal vapor diffusion with pentane to yield pure **19b** (0.296 g, 56%). Red solid. M.p. 164–167° (pentane/CH_2Cl_2). R_f (hexane/AcOEt 1:1) 0.52. UV/VIS (MeCN; *Figs. 11* and *12*): max. 484 (4.35), 355 (4.07), 274 (sh, 4.05), 242 (4.21), 206 (4.41); min. 407 (3.80), 310 (3.76), 234 (4.20). IR (KBr): 2944*m*, 2910*m*, 2853*m*, 2810*w* and 2713*w* (CHO), 1722v*s* (C=O, ester), 1665v*s* (C=O, aldehyde), 1620v*s*, 1592*s*, 1561*m*, 1541*s*, 1489v*s*, 1432v*s*, 1414v*s*, 1389v*s*, 1353*s*, 1289v*s*, 1257v*s*, 1200v*s*, 1177*s*, 1144*m*, 1097v*s*, 1064v*s*, 1000*m*, 976*w*, 951*m*, 908*s*, 869*m*, 847*s*, 807*m*, 792*m*, 736*w*, 714*w*, 695*w*, 636*w*, 617*m*, 581*w*, 563*w*, 551*w*, 521*w*, 509*w*, 489*w*. ^{1}H-NMR (300 MHz, $CDCl_3$): 9.30 (*s*, CHO); 7.16 (*d*, $^3J(3,2) = 6.9$, H–C(3)); 6.33 (*d*, $^3J(2',1') = 13.0$, H–C(2')); 6.17 (*d*, $^3J(2,3) = 6.9$, H–C(2)); 6.12 (*s*, H–C(7 or 9)); 6.06 (*s*, H–C(9 or 7)); 5.26 (*d*, $^3J(1',2') = 13.0$, H–C(1')); 3.70 (*s*, COOMe); 2.81 (*s*, Me_2N); 2.04 (*d*, $^4J = 0.9$, Me); 1.88 (*d*, $^4J = 1.0$, Me); 1.64 (*s*, Me–C(10)). ^{13}C-NMR (75 MHz, $CDCl_3$): 191.85 (*d*, CHO); 168.42 (*s*, *C*OOMe); 148.45 (*d*); 146.92 (*s*); 145.77 (*d*); 141.98 (*s*); 139.34 (*s*); 134.45 (*s*); 131.99 (*s*); 130.70 (*s*); 130.06 (*d*); 129.51 (*d*); 123.01 (*s*); 122.30 (*s*); 116.47 (*d*); 98.27 (*d*); 51.85 (*q*, COO*Me*); 40.74 (2*q*, Me_2N); 24.95 (*q*); 21.29 (*q*); 18.93 (*q*). EI-MS: 351 (100, $M^{+\bullet}$), 336 (7, $[M - Me]^+$), 322 (9, $[M - CHO]^+$), 308 (21, $[M - MeN{=}CH_2]^+$), 264 (6), 248 (7), 203 (29), 189 (7), 165 (9), 136 (10), 123 (7), 105 (11), 57 (16). Anal. calc. for $C_{22}H_{25}NO_3$ (351.45): C 75.19, H 7.17, N 3.99; found: C 75.26, H 7.16, N 3.91.

2.3. *1-[(1*E*)-2-(Dimethylamino)ethenyl]-5,6,8,10-tetramethylheptalene-4-carboxaldehyde* (**20b**) and *1-[(1*E*)-2-(Dimethylamino)ethenyl]-5,6,8,10-tetramethylheptalene-2-carboxaldehyde* (**18a**). Under Ar, *N,N,N′,N′,N″,N″*-hexamethylmethanetriamine (TDMAM; 0.26 ml, 1.50 mmol) was heated in DMF (5 ml) at 100°. At this temp., the solid DBS mixture **4b**/**4a** (0.126 g, 0.50 mmol) was added all at once (→ immediately red soln.). Stirring at 100° was continued for 45 min. The usual workup of the cooled mixture after dilution with ^{t}BuOMe gave a red oil, which was subjected to CC (Al_2O_3, act. IV, hexane/Et_2O 10:1 → 1:10): two orange fractions, the faster moving delivering **20b** (50.3 mg, 33%) and the slower one **18a** (54.2 mg, 35%).

Data of **18a**: See *2.1*.

Data of **20b**: Dark red, metallically shiny crystals. M.p. 138–142° (hexane/Et_2O). R_f (hexane/AcOEt 1:1) 0.82. UV/VIS (MeCN; *Figs. 10* and *12*): max. 467 (4.35), 391 (3.95), 319 (3.86), 276 (4.12), 234 (sh, 4.23); min. 400 (3.95), 345 (3.78), 307 (3.85), 262 (4.09). IR (KBr): 2963*m*, 2929*m*, 2908*m*, 2853*m*, 2810*w* and 2711*w* (C–H, aldehyde), 1665v*s* (C=O), 1619v*s*, 1595v*s*, 1541*s*, 1484v*s*, 1429*s*, 1415*s*, 1387v*s*, 1354*s*, 1287*s*, 1216*s*, 1203*s*, 1174*s*, 1146*w*, 1134*m*, 1104v*s*, 1037*m*, 991*w*, 949*m*, 909*m*, 901*m*, 887*m*, 852*s*, 834*m*, 808*w*, 795*m*, 773*w*, 720*w*, 705*w*, 660*w*, 636*w*, 608*m*, 575*w*, 546*w*, 513*w*, 482*w*. ^{1}H-NMR (300 MHz, (D_6)acetone): 9.38 (*s*, CHO); 7.06 (*d*, $^3J(3,2) = 7.0$, H–C(3)); 6.42 (*d*, $^3J(2',1') = 13.0$, H–C(2')); 6.14 (*d*, $^3J(2,3) = 7.0$, H–C(2)); 6.07 (*s*, H–C(7 or 9)); 6.05 (*s*, H–C(9 or 7)); 5.29 (*d*, $^3J(1',2') = 13.0$, H–C(1')); 2.82 (*s*, Me_2N); 1.96 (*d*, $^4J = 1.2$, Me); 1.95 (*s*, Me); 1.89 (*d*, $^4J = 1.4$, Me); 1.58 (*s*, Me). ^{13}C-NMR (75 MHz, (D_6)acetone): 193.69 (*d*, CHO); 149.21 (*d*); 147.57 (*s*); 146.78 (*d*); 139.00 (*s*); 138.51 (*s*); 135.74 (*s*); 133.92 (*s*); 131.03 (*d*); 129.90 (*d*); 129.26 (*s*); 127.25 (*s*); 126.60 (*s*); 116.65 (*d*); 97.96 (*d*); 40.80 (2*q*, Me_2N); 24.95 (*q*); 21.11 (*q*); 18.97 (*q*); 14.70 (*q*). EI-MS: 307 (100, $M^{+\bullet}$), 292 (10, $[M - Me]^+$), 278 (8, $[M - CHO]^+$), 264 (23, $[M - MeN{=}CH_2]^+$), 248 (8), 212 (9), 189 (7), 165 (7), 153.5 (8, M^{2+}), 109 (9), 58 (7). Anal. calc. for $C_{21}H_{25}NO$ (307.44): C 82.04, H 8.20, N 4.56; found: C 81.87, H 8.16, N 4.55.

3. *Formation of the 2-(Heptalenylmethylene)propanedinitriles.* 3.1. *2-[(1,5,6,8,10-Pentamethylheptalen-2-yl)methylene]propanedinitrile* (**21a**) *and 2-[(1,5,6,8,10-pentamethylheptalen-4-yl)methylene]propanedinitrile* (**21b**). The DBS mixture **4b**/**4a** (0.590 g, 2.34 mmol) and propanedinitrile (0.216 g, 3.37 mmol) were dissolved CH_2Cl_2 (30 ml) and cooled to 0°. At 0°, a soln. of $TiCl_4$ (0.67 ml, 6.08 mmol) in CH_2Cl_2 (10 ml) was added drop by drop under vigorous stirring (yellow soln. → dark green and turbid). Afterwards, a soln. of pyridine (2.07 ml, 25.7 mmol) in CH_2Cl_2 was added under continuous cooling and

stirring (→ brown suspension). The cooling was removed and stirring was continued for an additional 1 hour. Then, 1M aq. HCl (10 ml) was added, which led to dissolution of the suspended matter. The now cleared two-phase mixture was worked up in the usual manner. The obtained red oil was purified by CC (SiO_2, hexane/Et_2O 10:1): **21a**/**21b** (0.605 g, 86%), ratio 75:25 (by ^{1}H-NMR). Red solid.

Data of **21a**[13]): Orange prisms. M.p. 152–154° (EtOH). R_f (hexane/AcOEt 10:1) 0.41. UV/VIS (MeCN): max. 430 (3.28), 321 (4.35), 241 (4.18); min. 391 (3.19), 272 (4.03), 226 (4.14). IR (KBr): 3049*w*, 2972*m*, 2944*m*, 2912*m*, 2854*w*, 2226*s* (C≡N), 1648*w*, 1612*m*, 1563v*s*, 1442*m*, 1374*m*, 1359*m*, 1312*m*, 1278*m*, 1211*m*, 1121*w*, 1025*w*, 934*w*, 870*w*, 841*m*, 784*m*, 631*w*, 609*w*, 590*w*, 518*w*. ^{1}H-NMR (300 MHz, $CDCl_3$): 7.76 (*s*, H–C(2)); 6.85 (*d*, ^3J = 11.7, H–C(3′ or 4′)); 6.47 (*d*, ^3J = 11.7, H–C(4′ or 3′)); 6.11 (*s*, H–C(7′ or 9′)); 6.00 (*s*, H–C(9′ or 7′)); 2.17 (*s*, Me); 1.99 (*d*, ^4J = 1.2, Me); 1.98 (*d*, ^4J = 1.3, Me); 1.74 (*s*, Me); 1.70 (*s*, Me). ^{13}C-NMR (75 MHz, $CDCl_3$): 155.96 (*d*); 150.05 (*s*); 139.31 (*s*); 136.45 (*d*); 136.12 (*s*); 133.41 (*s*); 131.20 (*s*); 130.26 (*s*); 130.06 (*d*); 129.71 (*d*); 129.41 (*s*); 129.19 (*s*); 125.46 (*d*); 114.51 (*s*, CN); 112.55 (*s*, CN); 82.59 (*s*); 25.00 (*q*); 21.99 (*q*); 20.77 (*q*); 18.00 (*q*); 17.30 (*q*). EI-MS: 300 (100, $M^{+\bullet}$), 285 (52, $[M - Me]^+$), 270 (36, $[M - 2\,Me]^{+\cdot}$), 260 (21, $[M - MeC{\equiv}CH]^+$), 255 (16, $[M - 3\,Me]^+$), 246 (15, $[M - MeC{\equiv}CMe]^+$), 198 (27), 184 (98 $[M - MeC{\equiv}CCH{=}C(CN)_2]^+$), 169 (14), 123 (25), 105 (18), 69 (17), 57 (18). Anal. calc. for $C_{21}H_{20}N_2$ (300.41): C 83.96, H 6.71, N 9.33; found: C 83.90, H 6.65, N 9.25.

Data of **21b**: Red crystals. M.p. 110–112° (EtOH). R_f (hexane/AcOEt 10:1) 0.41. ^{1}H-NMR (300 MHz, $CDCl_3$): 7.63 (*s*, H–C(2)); 7.09 (*d*, ^3J(3′,2′) = 6.2, H–C(3′)); 6.27 (br. *d*, ^3J(2′,3′) = 6.2, H–C(2′)); 6.09 (*s*, H–C(7′ or 9′)); 5.99 (*s*, H–C(9′ or 7′)); 2.07 (*m*, Me); 2.00 (*d*, ^4J = 1.3, Me); 1.98 (*d*, ^4J = 1.3, Me); 1.79 (*s*, Me); 1.71 (*s*, Me). EI-MS: 300 (67, $M^{+\bullet}$), 285 (36, $[M - Me]^+$), 270 (25, $[M - 2\,Me]^{+\cdot}$), 260 (14, $[M - MeC{\equiv}CH]^+$), 255 (9, $[M - 3\,Me]^+$), 246 (10, $[M - MeC{\equiv}CMe]^+$), 198 (23), 184 (100, $[M - MeC{\equiv}CCH{=}C(CN)_2]^+$), 169 (14), 165 (8), 115 (8), 86 (9).

3.2. *Methyl 4-(2,2-Dicyanoethenyl)-1-[(1*E*)-2-(dimethylamino)ethenyl]-6,8,10-trimethylheptalene-5-carboxylate* (**23b**). As described in *3.1.*, with **19b** (140.6 mg, 0.40 mmol), **1** (37 mg, 0.56 mmol), $TiCl_4$ (1.04 mmol), and pyridine (0.36 ml, 4.4 mmol) in CH_2Cl_2 (5 ml). The finally blue mixture was worked up to yield a blue oil, which was subjected to CC (Al_2O_3, act. IV, hexane/Et_2O 1:1 → 1:3). The solid, obtained from the violet fraction, was dissolved in a small amount of CH_2Cl_2 and then re-solidified by addition of pentane and dried under h.v.: **23b** (75.7 mg, 47%). Green, metallically shiny needles. M.p. 195–198° (pentane/CH_2Cl_2). R_f (hexane/AcOEt 1:1) 0.39. UV/VIS (MeCN; *Figs. 11* and *13*): max. 602 (4.62), 416 (3.88), 299 (4.03), 236 (sh, 4.32), 211 (4.43); min. 465 (3.64), 367 (3.70), 283 (4.00). IR (KBr): 2946*w*, 2911*w*, 2855*w*, 2207v*s* (C≡N), 1713*s* (C=O), 1617v*s*, 1531*m*, 1473v*s*, 1432v*s*, 1416*s*, 1398*s*, 1353v*s*, 1341v*s*, 1263v*s*, 1227v*s*, 1198v*s*, 1104*s*, 1054*m*, 999*w*, 951*m*, 935*s*, 892*s*, 867*m*, 846*m*, 812*m*, 798*m*, 733*w*, 718*w*, 650*w*, 623*w*, 595*m*, 566*w*, 515*w*, 478*w*. ^{1}H-NMR (300 MHz, $CDCl_3$): 7.46 (*d*, ^3J(3,2) = 7.6, H–C(3)); 7.16 (*s*, H–C(1″)); 6.47 (*d*, ^3J(2′,1′) = 12.7, H–C(2′)); 6.18 (*s*, H–C(7 or 9)); 6.15 (*d*, ^3J(2,3) = 7.6, H–C(2)); 6.04 (*s*, H–C(9 or 7)); 5.39 (*d*, ^3J(1′,2′) = 12.7, H–C(1′)); 3.75 (*s*, COOMe); 2.91 (*s*, Me_2N); 2.06 (*d*, ^4J = 1.1, Me); 1.88 (*d*, ^4J = 1.2, Me); 1.65 (*s*, Me). ^{13}C-NMR (75 MHz, $CDCl_3$): 166.82 (*s*, *C*OOMe); 159.51 (*d*); 151.03 (*s*); 148.44 (*d*); 144.57 (*s*); 143.97 (*d*); 140.12 (*s*); 131.78 (*s*); 130.69 (*s*); 129.51 (*d*); 128.35 (*d*); 127.88 (*s*); 123.45 (*s*); 121.49 (*s*); 117.38 (*d*); 116.41 (*s*, CN); 114.37 (*s*, CN); 99.61 (*d*); 72.09 (*s*); 52.07 (*q*, COO*Me*), 41.22 (br. 2*q*, Me_2N), 24.82 (*q*); 20.78 (*q*); 18.86 (*q*); EI-MS: 399 (100, $M^{+\bullet}$), 384 (54, $[M - Me]^+$), 351 (36), 340 (14), 336 (8), 325 (9), 308 (11), 297 (27), 290 (10), 239 (9), 238 (11), 95 (15), 86 (19), 84 (31), 49 (27). Anal. calc. for $C_{25}H_{25}N_3O_2$ (399.49): C 75.16, H 6.31, N 10.52; found: C 74.86, H 6.33, N 10.28.

The structure of **23b** was finally established by an X-ray crystal-structure analysis (*Fig. 4*, *Tables 1*, *2*, and *8*).

3.3. *2-{[1-[(1*E*)-2-(Dimethylamino)ethenyl]-5,6,8,10-tetramethylheptalen-4-yl]methylene}propanedinitrile* (**24b**). As described in *3.1.*, with **20b** (88.0 mg, 0.29 mmol), **1** (26.4 mg, 0.40 mmol), $TiCl_4$ (0.75 mmol), and then pyridine (0.26 ml, 3.2 mmol) in CH_2Cl_2 (3 ml). The finally blue mixture was

---

[13]) Crystalline trace amounts of **21a** and **21b** could be isolated from enriched mixtures of both due to their different colors. In the course of these experiments, we learned that **21b** is quite sensible to daylight and forms **21a**. Heating of **21a** at 100° in toluene under rigorous exclusion of light enriched **21b** up to 80% – a possibility to isolate trace amounts of **21b**.

worked up to yield a blue oil, which was subjected to CC (Al_2O_3, act. IV, hexane/Et_2O 2:1). The product was precipitated from the blue concentrated fraction by addition of hexane, washed with hexane, and dried under h.v.: **24b** (65.1 mg, 63%). Green, metallically shiny prisms. M.p. 207–209° (hexane/Et_2O). R_f (hexann/AcOEt 1:1) 0.67. UV/VIS (MeCN; *Figs. 10* and *13*): max. 614 (4.61), 432 (3.88), 347 (sh, 3.67), 316 (sh, 3.92), 297 (3.99), 240 (4.35), 216 (4.32); min. 476 (3.70), 372 (3.50), 276 (3.92), 225 (4.30), 211 (4.32). IR (KBr): 2964*w*, 2932*m*, 2911*m*, 2817*w*, 2211v*s* (C≡N), 2194*s* (C≡N), 1610v*s*, 1599v*s*, 1538*s*, 1469v*s*, 1433v*s*, 1401v*s*, 1364v*s*, 1343v*s*, 1271v*s*, 1245*s*, 1211v*s*, 1184*s*, 1173*s*, 1161*s*, 1135*s*, 1108v*s*, 1038*m*, 1021*m*, 976*m*, 937*m*, 894*s*, 882*s*, 853*s*, 841*s*, 801*w*, 785*w*, 722*w*, 698*w*, 662*w*, 628*w*, 608*m*, 587*m*, 567*w*, 559*w*, 512*w*, 469*w*, 457*w*. ^{1}H-NMR (600 MHz, $CDCl_3$): 7.47 (*d*, $^3J(3',2') = 7.9$, H–C(3′)); 7.46 (*s*, H–C(2)); 6.55 (*d*, $^3J(2'',1'') = 12.7$, H–C(2″)); 6.14 (*d*, $^3J(2',3') = 7.9$, H–C(2′)); 6.10 (*s*, H–C(7′ or 9′)); 6.03 (*s*, H–C(9′ or 7′)); 5.35 (*d*, $^3J(1'',2'') = 12.7$, H–C(1″)); 2.91 (*s*, Me_2N); 2.00 (*s*, Me); 1.90 (*s*, Me); 1.82 (*s*, Me); 1.61 (*s*, Me). ^{13}C-NMR (150 MHz, $CDCl_3$): 158.39 (*d*); 151.00 (*s*); 148.34 (*d*); 141.14 (*d*); 139.32 (*s*); 134.06 (*s*); 133.20 (*s*); 132.55 (*s*); 130.29 (*d*); 129.69 (*d*); 129.64 (*s*); 126.34 (*s*); 125.74 (*s*); 117.56 (*d*); 117.06 (*s*, CN); 115.40 (*s*, CN); 99.19 (*d*); 71.13 (*s*); 41.27 (br. *q*, Me_2N); 24.99 (*q*); 21.03 (*q*); 19.02 (*q*); 15.51 (*q*). GC/EI-MS: 355 (100, $M^{+\bullet}$), 340 (81, $[M - Me]^+$), 325 (12), 310 (15), 296 (19), 283 (12), 269 (15), 260 (20), 253 (48), 238 (37), 224 (12), 209 (17), 193 (16), 179 (19), 177.5 (33, M^{2+}), 165 (15), 141 (11), 126 (15), 109 (16), 95 (48), 94 (27), 58 (26).

The structure of **24b** was finally established by an X-ray crystal-structure analysis (*Fig. 5*, *Tables 1*, *2*, and *8*).

3.4. *2-{[1-[(1*E*)-2-(Dimethylamino)ethenyl]-5,6,8,10-tetramethylheptalen-2-yl]methylene}propanedinitrile* (**26a**) *and 2-{(2*E*)-2-{(2*E*)-2-[(Dimethylamino)methylene]-5,6,8,10-tetramethylheptalen-1(2*H*)-ylidene}ethylidene}propanedinitrile* (**27**). As described in *3.1.*, with **18a** (0.615 g, 2.00 mmol) and **1** (0.185 g, 2.80 mmol) in CH_2Cl_2 (20 ml), $TiCl_4$ (5.2 mmol), and pyridine (1.8 ml, 22.0 mmol). The initially red CH_2Cl_2 soln. turned to dark green with $TiCl_4$ and finally to violet with pyridine. The crude product was separated by CC (SiO_2, hexane/AcOEt 2:1 → 1:2). The first wine-red fraction delivered, after drying under h.v., **26a** (0.119 g, 17%), and the second violet fraction, after drying under h.v., **27** (0.152 g, 21%).

Data of **26a**: Green, metallically shiny platelets. M.p. 232–235° (pentane/CH_2Cl_2). R_f (hexane/AcOEt 1:1) 0.61. UV/VIS (MeCN; *Fig. 14*): max. 544 (4.53), 396 (3.99), 318 (4.23), 265 (4.19), 228 (4.35), 207 (4.35); min. 448 (3.63), 358 (3.78), 293 (4.11), 250 (4.14), 218 (4.33), 205 (4.35). IR (KBr): 2970*w*, 2936*w*, 2910*w*, 2855*w*, 2813*w*, 2204v*s* (C≡N), 1607v*s*, 1515v*s*, 1488v*s*, 1444*m*, 1429*s*, 1417*s*, 1399*m*, 1366*s*, 1332*s*, 1290*s*, 1275*s*, 1236v*s*, 1167*m*, 1112*s*, 1068*m*, 1027*w*, 996*w*, 964*w*, 925*m*, 862*w*, 843*m*, 793*m*, 760*w*, 729*w*, 696*w*, 675*w*, 656*w*, 628*w*, 615*w*, 593*w*, 553*w*, 515*w*, 484*w*, 466*w*. ^{1}H-NMR (300 MHz, $CDCl_3$): 7.62 (*s*, H–C(2)); 6.94 (*d*, $^3J = 11.5$, H–C(3′)); 6.68 (*d*, $^3J(2'',1'') = 12.2$, H–C(2″)); 6.14 (*s*, H–C(7′ or 9′)); 6.12 (*d*, $^3J = 11.5$, H–C(4′)); 6.08 (*s*, H–C(9′ or 7′)); 5.42 (*d*, $^3J(1'',2'') = 12.2$, H–C(1″)); 3.00 (*s*, Me_2N); 2.01 (*d*, $^4J = 1.0$, Me); 1.87 (*d*, $^4J = 1.1$, Me); 1.74 (*s*, Me); 1.61 (*s*, Me). ^{13}C-NMR (75 MHz, $CDCl_3$): 154.13 (*s*); 152.28 (*d*); 151.55 (*d*); 138.20 (*s*); 134.55 (*s*); 134.28 (*s*); 130.33 (*d*); 129.94 (*s*); 129.74 (*d*); 129.27 (*d*); 128.08 (*s*); 127.12 (*s*); 126.22 (*d*); 120.86 (*s*); 118.02 (*s*, CN); 115.91 (*s*, CN); 95.79 (*d*); 69.15 (*s*); 41.46 (br. 2*q*, Me_2N), 24.95 (*q*); 21.21 (*q*); 18.04 (*q*); 17.72 (*q*). EI-MS: 355 (100, $M^{+\bullet}$), 340 (49, $[M - Me]^+$), 315 (19), 301 (13), 283 (9), 252 (8), 227 (6), 184 (28, $[M - Me_2NCH{=}CHC{\equiv}CCH{=}C(CN)_2]^{+\bullet}$), 149 (42), 123 (14), 105 (12), 71 (11), 69 (11), 57 (27), 43 (22), 41 (20).

The structure of **26a** was finally established by an X-ray crystal-structure analysis (*Fig. 7*, *Tables 3*, *4*, and *8*).

Data of **27**: Green, metallically shiny prisms. M.p. 229–233° (pentane/CH_2Cl_2). R_f (hexane/AcOEt 1:1) 0.52. UV/VIS (MeCN): max. 558 (4.50), 394 (4.03), 312 (4.28), 294 (sh, 4.26), 273 (sh, 4.16), 218 (4.32); min. 451 (3.52), 353 (3.76), 253 (4.09), 215 (4.32). IR (KBr): 2972*w*, 2936*m*, 2911*m*, 2204v*s* (C≡N), 1591*s*, 1515v*s*, 1482*s*, 1447*m*, 1415*s*, 1398*s*, 1361*s*, 1342*s*, 1297*s*, 1270*s*, 1223v*s*, 1124*s*, 1096*m*, 1071*m*, 1054*w*, 1028*w*, 994*m*, 938*s*, 865*m*, 849*m*, 823*w*, 809*w*, 785*w*, 726*w*, 686*w*, 653*w*, 623*m*, 606*w*, 589*w*, 550*w*, 512*w*. ^{1}H-NMR (300 MHz, $CDCl_3$): 7.16 (*s*, H–C(1″)); 7.07 (*d*, $^3J(2,3) = 12.6$, H–C(2)); 6.39 (*d*, $^3J = 11.6$, H–C(3′)); 6.26 (*d*, $^3J(3,2) = 12.6$, H–C(3)); 6.12 (*s*, H–C(7′ or 9′)); 6.09 (*s*, H–C(9′ or 7′)); 5.81 (*d*, $^3J = 11.6$, H–C(4′)); 3.32 (*s*, Me_2N); 2.02 (*d*, $^4J = 1.1$, Me); 1.88 (*d*, $^4J = 1.2$, Me); 1.74 (*s*, Me); 1.59 (*s*, Me). ^{13}C-NMR (75 MHz, $CDCl_3$): 159.03 (*s*); 154.50 (*d*); 150.34 (*d*); 138.28 (*s*); 135.07 (*s*); 133.85 (*s*); 129.36 (*d*); 129.16 (*d*); 128.90 (*s*); 127.54 (*s*); 126.98 (*d*); 126.46 (*s*); 124.86 (*d*); 117.28 (*s*, CN); 115.20 (*s*, CN);

111.45 (*s*); 108.58 (*d*); 67.69 (*s*); 44.86 (2*q*, Me_2N); 24.86 (*q*); 21.66 (*q*); 18.07 (*q*); 17.81 (*q*). EI-MS: 355 (66, $M^{+\bullet}$), 340 (26, $[M - Me]^+$), 325 (7, $[M - 2\,Me]^{+\bullet}$), 297 (9), 295 (9), 234 (12), 213 (13), 184 (100, $[M - Me_2NCH{=}C{=}CCH{=}C(CN)_2]^{+\bullet}$), 169 (42), 165 (12), 153 (11), 141 (11), 129 (21), 121 (12), 115 (12), 82 (16), 42 (17). Anal. calc. for $C_{24}H_{25}N_3$ (355.49): C 81.09, H 7.09, N 11.82; found: C 81.26, H 6.81, N 11.94.

The structure of **27** was finally established by an X-ray crystal-structure analysis (*Fig. 8*, *Tables 3*, *4*, and *8*).

4. *X-Ray Crystal-Structure Determinations of Compounds* **13b**, **18a**, **23b**, **24b**, **26a**, **27**, *and* **28b** (see *Table 8* and *Figs. 2–5* and *7–9*)[14]). All measurements for **13b** and **28b** were conducted at low-temperature with a *Rigaku-AFC5R* diffractometer [25] fitted to a 12 kW rotating-anode generator, while those for all other structures were made with a *Nonius-KappaCCD* area-detector diffractometer [26][27] equipped with an *Oxford-Cryosystems-Cryostream-700* cooler. Graphite-monochromated MoK_α radiation (λ 0.71073 Å) was used for all measurements. The intensities for each structure were corrected for *Lorentz* and polarization effects, but not for absorption. The data collection and refinement parameter are given in *Table 8*, views of the molecules are shown in *Figs. 2–5* and *7–9*.

Each structure was solved by direct methods with SHELXS97 [28] or SIR92 [29], which revealed the positions of all non-H-atoms. In **18a**, the aldehyde O-atom was disordered over two orientations which were related by a rotation of *ca.* 165° about the parent aldehyde C–C bond. The site-occupation factors of the disordered atoms were initially refined and then fixed, with a value for the major conformation of 0.77. The non-H-atoms of each structure were refined anisotropically. The H-atoms of **28b** were placed in the positions indicated by difference *Fourier* maps, and their positions were allowed to refine together with individual isotropic displacement parameters. All H-atoms in the remaining structures were placed in geometrically calculated positions and refined by using a riding model where each H-atom was assigned a fixed isotropic displacement parameter with a value equal to 1.2 U_{eq} of its parent atom. The Me substituents at C(5) and C(6) of **24b** were rotationally disordered with two equally occupied orientations of the H-atoms being located for each group.

Each structure was refined on *F* with full-matrix least-squares procedures, which minimized the function $\Sigma w(|F_o| - |F_c|)^2$. Corrections for secondary extinction were applied in all cases, except for **13b** and **18a**. Neutral-atom scattering factors for non-H-atoms were taken from [30a], and the scattering factors for H-atoms were taken from [31]. Anomalous dispersion effects were included in F_c [32]; the values for f' and f'' were those of [30b]. The values of the mass attenuation coefficients were those of [30c]. All calculations were performed with the teXsan crystallographic software package [33]. The crystallographic diagrams were drawn with ORTEPII [34].

REFERENCES

[1] S. Maillefer-El Houar, P. Uebelhart, A. Linden, H.-J. Hansen, *Helv. Chim. Acta* **2013**, *96*, 1488.
[2] P. Ott, H.-J. Hansen, *Helv. Chim. Acta* **2001**, *84*, 2670.
[3] P. Scheibe, S. Schneider, F. Dörr, E. Daltrozzo, *Ber. Bunsenges. Phys. Chem.* **1976**, *80*, 630.
[4] Z. A. Krasnaya, T. S. Stytsenko, *Russ. Chem. Bull.* **1983**, *32*, 780.
[5] K. A. Bello, L. Cheng, J. Griffiths, *J. Chem. Soc., Perkin Trans. 2* **1987**, 815.
[6] A. Asiri, *Bull. Korean Chem. Soc.* **2003**, *24*, 426.
[7] T. Landmesser, A. Linden, H.-J. Hansen, *Helv. Chim. Acta* **2008**, *91*, 265.
[8] G. L. Knaup, Ph.D. Thesis, University of Darmstadt, 1985; K. Hafner, N. Hock, G. L. Knaup, K.-P. Meinhardt, *Tetrahedron Lett.* **1986**, *27*, 1669.
[9] P. Uebelhart, P. Mohler, R.-A. Fallahpour, H.-J. Hansen, *Helv. Chim. Acta* **1995**, *78*, 1437.
[10] C. Hörndler, H.-J. Hansen, *Helv. Chim. Acta* **1997**, *80*, 2520.
[11] Y. Chen, R. W. Kunz, P. Uebelhart, R. H. Weber, H.-J. Hansen, *Helv. Chim. Acta* **1992**, *75*, 2447.

---

14) CCDC-915305–915311 contain the supplementary crystallographic data for this article. These data can be obtained free of charge from the *Cambridge Crystallographic Data Centre via* www.ccdc.cam.ac.uk/data_request/cif.

[12] A. A. S. Briquet, P. Uebelhart, H.-J. Hansen, *Helv. Chim. Acta* **1996**, *79*, 2282.
[13] R. H. Weber, P. Brügger, W. A. Arnold, P. Schönholzer, H.-J. Hansen, *Helv. Chim. Acta* **1987**, *70*, 1439.
[14] A. D. Batcho, W. Leimgruber, to *Hoffmann-La Roche Inc.,* US, U.S. Pat., 3 732 245, 08.05.1973; R. D. Clarke, D. B. Repke, *Heterocycles* **1984**, *22*, 195.
[15] K. Abou-Hadeed, Z. A. Molnar, P. Göksaltik, R. W. Kunz, A. Linden, H.-J. Hansen, *Helv. Chim. Acta* **2012**, *95*, 885.
[16] B. S. Ong, B. Keoshkerian, *J. Org. Chem.* **1984**, *49*, 5002.
[17] P. H. J. Ooms, M. A. Bertisen, H. W. Scheeren, R. J. F. Nivard, *J. Chem. Soc., Perkin Trans. 1* **1976**, 1538.
[18] S. V. Ley, J. Norman, W. P. Griffith, S. P. Marsden, *Synthesis* **1994**, 639.
[19] M. G. Ventelino, J. W. Coe, *Tetrahedron Lett.* **1994**, *35*, 219.
[20] J. Drew, M. Letellier, P. Morand, A. G. Szabo, *J. Org. Chem.* **1987**, *52*, 4047.
[21] a) S. R. Marder, C. B. Gorman, B. G. Tiemann, L.-P. Cheng, *J. Am. Chem. Soc.* **1993**, *115*, 3006; b) G. Bourhill, J.-L. Brédas, L.-T. Cheng, S. R. Marder, F. Meyers, J. P. Perry, B. G. Tiemann, *J. Am. Chem. Soc.* **1994**, *116*, 2619.
[22] L. Ulrich, H.-J. Hansen, H. Schmid, *Helv. Chim. Acta* **1970**, *53*, 1323; H. Heimgartner, L. Ulrich, H.-J. Hansen, H. Schmid, *Helv. Chim. Acta* **1971**, *54*, 2313; W. Sieber, H. Heimgartner, H.-J. Hansen, H. Schmid, *Helv. Chim. Acta* **1972**, *55*, 3005.
[23] W. Bernhard, P. Brügger, J. J. Daly, P. Schönholzer, R. H. Weber, H.-J. Hansen, *Helv. Chim. Acta* **1985**, *68*, 415.
[24] K. Hafner, G. L. Knaup, *Tetrahedron Lett.* **1986**, *27*, 1665.
[25] MSC/AFC Diffractometer Control Software, Molecular Structure Corporation, The Woodlands, Texas, 1991.
[26] R. Hooft, KappaCCD Collect Software, Nonius BV, Delft, The Netherlands, 1999.
[27] Z. Otwinowski, W. Minor, in 'Methods in Enzymology', Vol. 276, 'Macromolecular Crystallography, Part A', Eds. C. W. Carter Jr., and R. M. Sweet, Academic Press, New York, 1997, pp. 307 – 326.
[28] G. M. Sheldrick, *Acta Crystallogr., Sect. A* **2008**, *64*, 112.
[29] A. Altomare, G. Cascarano, C. Giacovazzo, A. Guagliardi, M. C. Burla, G. Polidori, M. Camalli, SIR92, *J. Appl. Crystallogr.* **1994**, *27*, 435.
[30] a) E. N. Maslen, A. G. Fox, M. A. O'Keefe, in 'International Tables for Crystallography', Ed. A. J. C. Wilson, Kluwer Academic Publishers, Dordrecht, 1992, Vol. C, Table 6.1.1.1, pp. 477 – 486; b) D. C. Creagh, W. J. McAuley, in 'International Tables for Crystallography', Ed. A. J. C. Wilson, Kluwer Academic Publishers, Dordrecht, 1992, Vol. C, Table 4.2.6.8, pp. 219 – 222; c) D. C. Creagh, J. H. Hubbell, in 'International Tables for Crystallography', Ed. A. J. C. Wilson, Kluwer Academic Publishers, Dordrecht, 1992, Vol. C, Table 4.2.4.3, pp. 200 – 206.
[31] R. F. Stewart, E. R. Davidson, W. T. Simpson, *J. Chem. Phys.* **1965**, *42*, 3175.
[32] J. A. Ibers, W. C. Hamilton, *Acta Crystallogr.* **1964**, *17*, 781.
[33] teXsan: Single Crystal Structure Analysis Software, Version 1.10, Molecular Structure Corporation, The Woodlands, Texas, 1999.
[34] C. K. Johnson, ORTEPII, Report ORNL-5138, Oak Ridge National Laboratory, Oak Ridge, Tennessee, 1976.

Received March 25, 2013